

## Review

# Two-dimensional nanomaterials beyond graphene for antibacterial applications: current progress and future perspectives

Linqiang Mei<sup>1,3</sup>, Shuang Zhu<sup>1</sup>, Wenyan Yin<sup>1</sup>✉, Chunying Chen<sup>2</sup>, Guangjun Nie<sup>2</sup>, Zhanjun Gu<sup>1,3</sup>✉, Yuliang Zhao<sup>2,3</sup>

1. CAS Key Laboratory for Biomedical Effects of Nanomaterials and Nanosafety, Institute of High Energy Physics, Chinese Academy of Sciences, Beijing 100049, China.
2. CAS Center for Excellence in Nanoscience, National Center for Nanoscience and Technology of China, Chinese Academy of Sciences, Beijing 100190, China.
3. College of Materials Science and Optoelectronic Technology, University of Chinese Academy of Sciences, Beijing 100049, China.

✉ Corresponding authors: Zhanjun Gu, zjgu@ihep.ac.cn; Wenyan Yin, yinwy@ihep.ac.cn.

© The author(s). This is an open access article distributed under the terms of the Creative Commons Attribution License (<https://creativecommons.org/licenses/by/4.0/>). See <http://ivyspring.com/terms> for full terms and conditions.

Received: 2019.08.27; Accepted: 2019.09.21; Published: 2020.01.01

## Abstract

The marked augment of drug-resistance to traditional antibiotics underlines the crying need for novel replaceable antibacterials. Research advances have revealed the considerable sterilization potential of two-dimension graphene-based nanomaterials. Subsequently, two-dimensional nanomaterials beyond graphene (2D NBG) as novel antibacterials have also demonstrated their power for disinfection due to their unique physicochemical properties and good biocompatibility. Therefore, the exploration of antibacterial mechanisms of 2D NBG is vital to manipulate antibacterials for future applications. Herein, we summarize the recent research progress of 2D NBG-based antibacterial agents, starting with a detailed introduction of the relevant antibacterial mechanisms, including direct contact destruction, oxidative stress, photo-induced antibacterial, control drug/metallic ions releasing, and the multi-mode synergistic antibacterial. Then, the effect of the physicochemical properties of 2D NBG on their antibacterial activities is also discussed. Additionally, a summary of the different kinds of 2D NBG is given, such as transition-metal dichalcogenides/oxides, metal-based compounds, nitride-based nanomaterials, black phosphorus, transition metal carbides, and nitrides. Finally, we rationally analyze the current challenges and new perspectives for future study of more effective antibacterial agents. This review not only can help researchers grasp the current status of 2D NBG antibacterials, but also may catalyze breakthroughs in this fast-growing field.

Key words: bacterial resistance, antibacterials, 2D NBG, antibacterial mechanisms, physicochemical properties

## 1. Introduction

The diseases caused by bacterial infections continue to be a major growing global health issue. According to statistics, pathogenic microorganisms including bacteria, fungi, viruses, protozoa, prions, and rickettsia caused millions of deaths all over the world annually [1-3]. Subsequently, the advent of antibiotics has effectively inhibited bacterial infections and saved countless lives, which are attributed to their natural properties and abilities to selectively kill

bacteria by disrupting cellular processes including protein synthesis, deoxyribonucleic acid (DNA) replication/repair, and cell-wall/membrane formation [4-7]. However, the overuse or misuse of traditional antibiotics has resulted in the emergence and rapid increase of multi-drug resistance “superbugs” day after day, consequently leading to extremely severe side effects [8-10]. It is estimated that if antibiotics resistance continues to emerge,

antibiotic-resistant infections will cause over ten million deaths annually and considerable global economy loss [11-13]. In addition, the formation of biofilm is another major obstacle that affects the bactericidal efficiency of traditional antibiotics [14-17]. Therefore, it is an urgent demand to search for low toxic antibiotics or develop new classes of alternative antibacterial to alleviate or address the looming crisis of bacterial resistance [18-21].

Recently, sparked by the rapid development of nanoscience and technology, substantial efforts have been aimed to develop versatile nanomaterials as novel antibacterial against various bacterial pathogens based on their extraordinary physicochemical characteristics [22-25]. Compared to traditional antibiotics, nanomaterials are less likely to trigger bacterial resistance owing to their good membrane permeability, benign biocompatibility and potential for multiple antibacterial actions [26-28]. In addition, 2D nanomaterials with large surface area and easy surface functionalization enable intimate interactions with bacteria membranes, which help in enhancing the antibacterial effect. Moreover, the 2D nanomaterials based antibacterial agents can be used at a low dose than traditional antibiotics, hence overcoming the problem of resistance and diminishing other undesirable side effects to some extent [29-31]. Significant progress has been achieved on the development of nanotechnology-based antibacterial nanoagents (graphene [32], noble metals [33], organic polymers [34], *etc.*) for combating multidrug resistance in bacteria through physical contact damage [35], oxidative stress [36], photo-induced antibacterial (such as photothermal therapy (PTT) [37], photocatalytic therapy (PTC) [38], and photodynamic therapy (PDT) [39]), controlled drug/metallic ions releasing [40], and multi-mode synergistic antibacterial [41]. Among various antibacterial nanoagents, 2D graphene and its derivatives have exhibited attractive applications in biomedicine (tumor diagnosis and therapy, neurological disorders treatment, and antibacterial) over the past decade [42-47], because of their intriguing biochemical properties, such as easy preparation and functionalization, high specific surface area, and good biocompatibility [48, 49]. Moreover, the investigations of graphene-based nanomaterials also facilitated the exploration of new two-dimensional nanomaterials beyond graphene (2D NBG) [50]. Fortunately, in recent years, 2D NBG has displayed attractive applications in the fields of catalysis, optical/electronic devices, and biomedicine, which could be attributed to favorable graphene-like physicochemical characteristics, such as large specific surface-area, ultrathin 2D nature, striking

light-to-heat capability, extraordinary photocatalytic features, facile surface modification, and relatively benign biocompatibility [51-53]. Particularly, recent advances reveal that 2D NBG has a robust antibacterial effect [54]. Moreover, these graphene-like nanomaterials-oriented antibacterials presented different types of antibacterial mechanisms [55]. To date, the family of 2D NBG nanomaterials have been enriched by many members, which include 2D layered transition metal dichalcogenides (TMDCs), transition metal oxides (TMDOs), graphitic carbon nitride (*g*-C<sub>3</sub>N<sub>4</sub>), black phosphorus (BP), layered double hydroxides (LDHs), transition metal carbides and nitrides (MXenes), and so on [52]. Currently, broad researches have been pursued on antibacterial applications of 2D NBG, such as direct interaction mechanism between 2D NBG and bacteria [56]. However, a comprehensive review with antibacterial progress, size/shape/phase structure and surface modification-oriented antibacterial advantages, future perspectives and challenges aiming specifically at 2D NBG for antibacterial is still rare. Therefore, it is obligatory to present a systematically summary of the recent research progress of 2D NBG in antibacterial field.

Herein, we provide a critical overview on the recent advances of 2D NBG-based antibacterial agents, specifically focusing on their dominant antibacterial mechanisms (schematic illustration in **Figure 1**). We first outline the underlying antibacterial mechanisms of 2D NBG and their derivatives as antibacterials based on the existing research studies. Then, a brief discussion of the relationship between the physicochemical characteristics of 2D NBG and antibacterial efficiency is presented. Furthermore, we enumerate some representative 2D NBG and their relevant antibacterial action. Finally, we provide our perspectives about the major obstacles in clinical translation of 2D NBG. We hope that this review can help researchers to understand the properties and antibacterial mechanisms of 2D NBG for antibacterial and draw public attention to develop novel efficient antibacterial strategies using the 2D NBG in the future.

## 2. Antibacterial Mechanisms and Physicochemical Characteristics Related Influencing Factors of 2D NBG

To the best of our knowledge, graphene-based nanomaterials with outstanding antibacterial activities based on their extraordinary characteristics, and predominant antibacterial mechanisms have been systematically reviewed by Luo's group in 2016 [57].

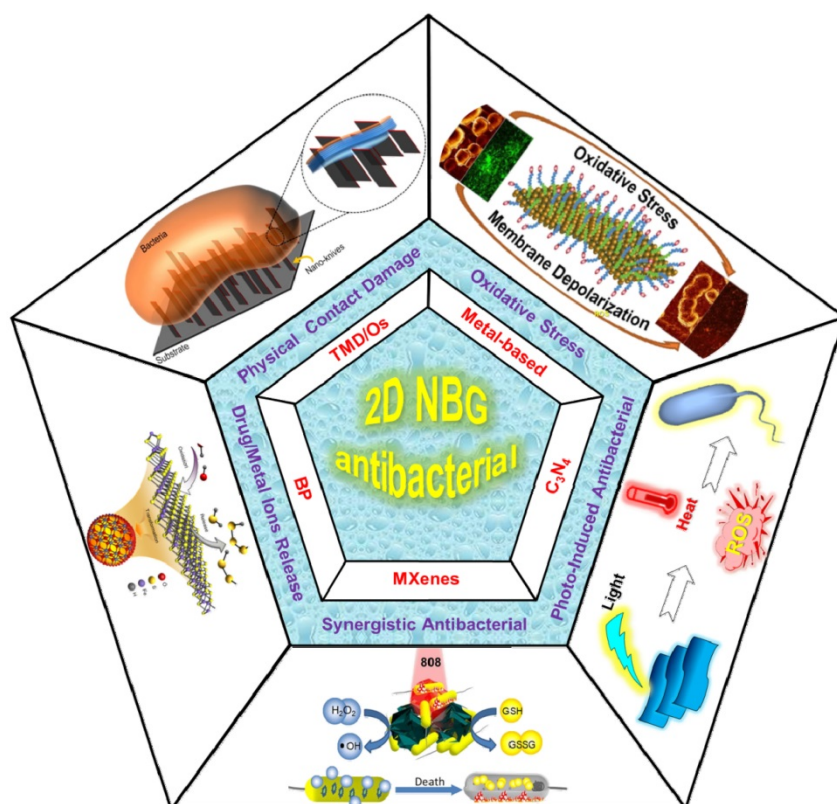


**Figure 1.** The existing antibacterial mechanisms and kinds of 2D NBG. Physical contact damage: Reproduced with permission from [58], copyright 2018 American Chemical Society. Oxidative stress: Reproduced with permission from [83], copyright 2016 American Chemical Society. Photo-induced generate heat or ROS for antibacterial. Controlled drug/metallic ions release: Reproduced with permission from [134], copyright 2018 Nature Publishing Group. Multi-mode Synergistic antibacterial: Reproduced with permission from [143], copyright 2016 American Chemical Society.

However, a thorough understanding of the underlying antibacterial mechanisms of 2D NBG remains in its infancy. Therefore, it is essential to summarize the existing antibacterial mechanisms of 2D NBG to manipulate antibacterial nanomaterials for future biomedical applications. According to recent achievements, we summarize that current antibacterial mechanisms of 2D NBG mainly include physical contact destruction, oxidative stress, photo-induced antibacterial, controlled drug/metallic ions release, and multi-mode synergistic antibacterial effects [54, 56]. In the following section, we will comprehensively clarify each antibacterial mechanism of 2D NBG and offer some hints to improve antibacterial effects.

## 2.1 Physical Contact Destruction

Several accumulated studies have demonstrated that the cell wall or membrane is an indispensable component in all bacteria, which is accountable for maintaining cell morphology, regulating osmotic pressure, and preventing infection [54]. It has been verified that Gram<sup>-</sup> and Gram<sup>+</sup> bacteria have different cell membrane structure (Figure 2A) [58-60]. The former possesses twain distinct lipoprotein membranes: a lipopolysaccharide coated inner cell

membrane and outer membrane, which is separated by a thin layer of peptidoglycan in the periplasmic space [59]. Conversely, Gram<sup>+</sup> bacteria are composed of single lipid bilayer cell membrane and multilayer thick peptidoglycan mesh outside of the cell membrane [60]. It has been confirmed that sharp edges of nanosheets (also regarded as “nanoknives”) were probably compromising bacterial membrane integrity upon physical contact, which could lead to the leakage of intracellular components, such as ribonucleic acid (RNA), DNA, phospholipids, and proteins, *etc.* [61]. This mechanism was initially proposed for graphene-based nanomaterials [35, 62]. In recent years, various 2D NBG such as MoS<sub>2</sub>, WS<sub>2</sub>, MoO<sub>3</sub>, RuO<sub>2</sub>, MnO<sub>2</sub>, and Bi<sub>2</sub>Se<sub>3</sub> have been used for physical contact disinfection because their sharp edges could damage cell wall or outer membrane [52]. For instance, Alimohammadi *et al.* reported that MnO<sub>2</sub> and MoS<sub>2</sub> nanosheets with blade-like shape show remarkable antibacterial effects towards *B. subtilis* and *E. coli* (Figure 2B) [58]. Intriguingly, they studied the antibacterial activities of randomly oriented and vertically aligned MoS<sub>2</sub>/MnO<sub>2</sub> nanosheets on graphene oxide or Ti<sub>3</sub>C<sub>2</sub> MXene nanosheets, and observed that vertically aligned MnO<sub>2</sub> nanosheets exhibit higher antibacterial activity than randomly

oriented nanosheets, which is ascribed to the sharp edges of vertically aligned  $\text{MnO}_2$  nanosheets drastic damaging the integrity of bacterial cell membrane (Figure 2C, D). Meanwhile, scanning electron microscope (SEM) images of the *B. subtilis* also verified that the sharp edge of  $\text{MnO}_2$  nanosheets can distinctly destroy bacterial morphology and ultimately kill bacteria, which also proved that 2D antibacterials probably mainly damage the peptidoglycan mesh of bacteria (Figure 2E). Similarly, Krishnamoorthy *et al.* revealed that the plate-like morphology of the as-prepared  $\text{MoO}_3$  functioned as “nanoknives” could kill bacteria through physical puncture of the outer bacterial wall [63, 64]. Furthermore, Liu *et al.* found that  $\text{WS}_2$  nanosheets cling more bacterial and show a robust antibacterial activity [65]. From the SEM and transmission electron microscope (TEM) images, they proposed that  $\text{WS}_2$  nanosheets with sharp edges could apparently damage the structural integrity of the bacterial

membrane, which is induced by the direct contact of bacteria and  $\text{WS}_2$  nanosheets. Besides, Jiang *et al.* developed a novel  $\text{Bi}_2\text{Se}_3$  nanodiscs through solvent thermal reaction for selectively treating Gram+ bacterial infections [66]. They found that  $\text{Bi}_2\text{Se}_3$  nanodiscs mainly damage bacterial wall/membrane by binding with lipoteichoic acid of Gram+ bacteria. It is worth noting that theoretical simulation results revealed that the physical contact destruction action of graphene nanosheets mainly depends on their sizes [67-70]. However, it is not clear whether the size or other physicochemical properties of 2D NBG will affect their antibacterial activity. Therefore, physical contact destruction as one of the most common antibacterial mechanisms should be further studied. And the combination of theoretical simulation with experiment to deeply explore the effect of nanomaterial physicochemical properties on antibacterial activity is also recommended.

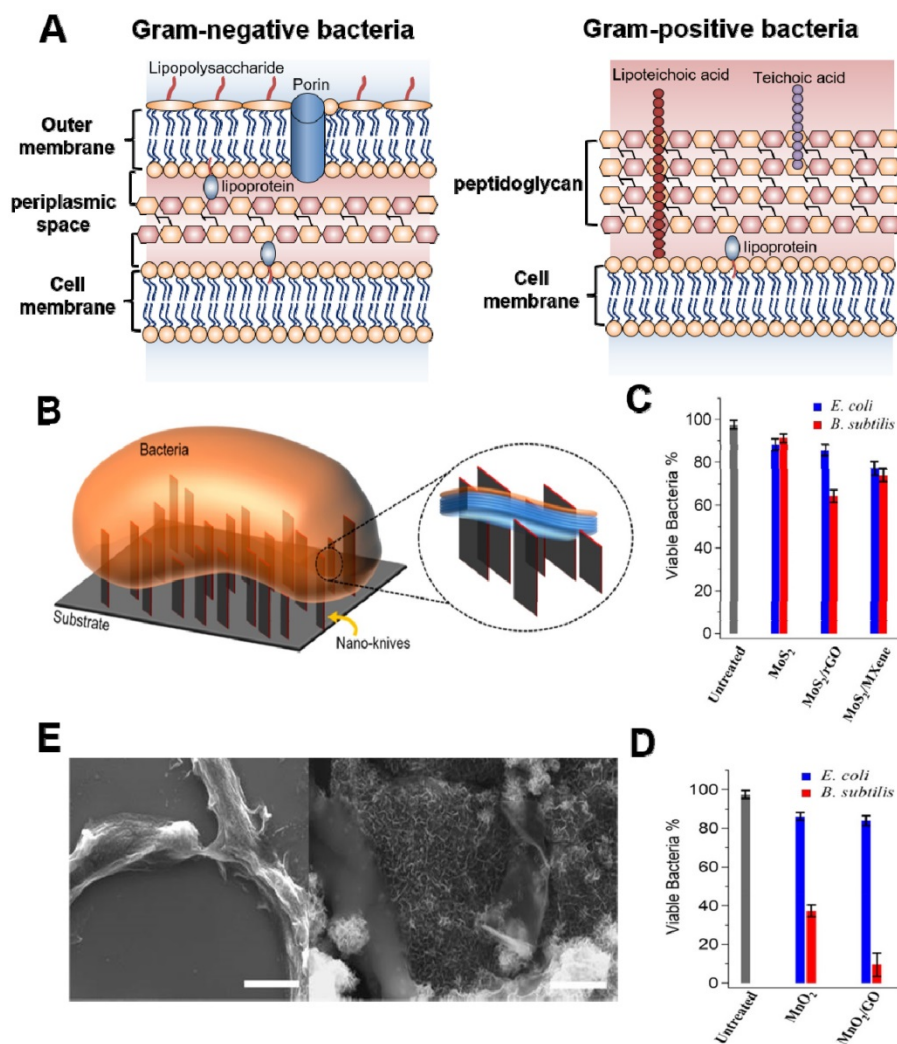


**Figure 2.** (A) General membrane ultrastructure of Gram- and Gram+ bacterial species. (B) Schematic representation of direct physical interaction of the bacterial surface with sharp edges of vertically aligned nanosheets onto a substrate. Antibacterial activities of (C)  $\text{MoS}_2$  and (D)  $\text{MnO}_2$  nanosheets against *E. coli* and *B. subtilis*. (E) SEM images of the *B. subtilis* bacteria treated with  $\text{MnO}_2$  and  $\text{MnO}_2/\text{GO}$  nanomaterials for 3 h in dark. Reproduced with permission from [58], copyright 2018 American Chemical Society.

## 2.2 Oxidative Stress Antibacterial

Oxidative stress can impede bacterial metabolism and continuously damage essential cellular functions, causing bacteria inactivation, and eventually killing bacteria [71, 72]. Therefore, the generation of oxidative stress is one of the widely accepted antibacterial methods. In general, 2D nanomaterials-mediated oxidative stress mainly includes reactive oxygen species (ROS)-dependent and ROS-independent oxidative stress.

### 2.2.1 ROS-Dependent Oxidative Stress

ROS-dependent oxidative stress is triggered by excessive accumulation of intracellular ROS, such as hydrogen peroxide ( $H_2O_2$ ), hydroxyl radicals ( $\bullet OH$ ), superoxide anions ( $\bullet O_2^-$ ), and singlet molecular oxygen ( $^1O_2$ ) under external/internal stimulus factors. Previous studies have demonstrated that graphene and its ramifications can generate ROS [8]. In general, an excessive amount of ROS not only causes direct damage to the bacterial structure by breaking DNA single strand but also leads to hyperoxidation of intracellular components. Recently, 2D NBG has been found to exert antibacterial performances through the production of ROS under light-dependent or light-independent stimulus factors. Several cumulative studies have documented that 2D  $MoS_2$  nanosheets with supramolecular self-assembly property could selectively produce ROS in a target cell rather than control cells, which is beneficial for their further biomedical application [73]. To verify the ROS-dependent oxidative stress, Karunakaran *et al.* used different thiol surfactant molecules to exfoliate and functionalize 2H- $MoS_2$  (H stands for hexagonal) nanosheets for enhancing the antibacterial effect (**Figure 3A**) [74]. By monitoring ROS levels using Ellman's assay, they found that 2H- $MoS_2$  nanosheets with suitable conduction band could incur more loss of glutathione (GSH) when compared to 1T- $MoS_2$  (T is trigonal) nanosheets (**Figure 3B**). Subsequently, they used different scavengers to ascertain the ROS type and found that  $H_2O_2$  is the dominant ROS (**Figure 3C**). Moreover, they used fluorescent probe 2',7'-dichlorofluorescein diacetate (DCFDA) to estimate the amount of intracellular ROS, and the results revealed that positively charged 2H- $MoS_2$  nanosheets can effectively attach to the bacterial surface and generate more ROS. In contrast, the negatively charged 2H- $MoS_2$  nanosheets with non-interactive property produced less ROS in bacteria. Therefore, due to the different semiconducting property of 2H and 1T phase, when compared to 1T- $MoS_2$ , the ROS-dependent oxidative stress is more obvious in 2H- $MoS_2$  nanosheets. Furthermore, the higher antibacterial capacity of

exfoliated 1T-phase TMDCs (including  $MoS_2$ ,  $WS_2$ ,  $MoSe_2$ ) nanosheets is also attributed to the production of ROS [75, 76]. In addition, Xiong *et al.* demonstrated that BP nanosheets can also strikingly kill *E. coli* and *B. subtilis* through ROS-dependent oxidative stress and membrane damage mechanism [77]. These studies not only partially verified the generation of ROS in bacteria, but also proved that ROS-dependent oxidative stress is an important antibacterial process.

### 2.2.2 ROS-Independent Oxidative Stress

Although the above-mentioned reviews underline the crucial role of ROS-dependent oxidative stress, several studies have revealed that ROS-independent oxidative stress also possesses a favorable bactericidal effect. In detail, ROS-independent oxidative stress mainly damages or oxidizes cellular structure and components (such as lipids, proteins, and DNA) by nanomaterials-induced direct oxidation rather than ROS production [78, 79]. GSH, a ubiquitous antioxidant *in vivo*, not only can serve as an intracellular redox state indicator but also can indicate the oxidative stress antibacterial effect owing to its easy oxidation into glutathione disulfide (GSSG) [80]. In 2008, Alvarez's group firstly proposed this antibacterial mechanism and they observed that the antibacterial ability of fullerene ( $nC_{60}$ ) does not rely on light and oxygen, which are the two conditions essential for ROS generation [81]. Similarly, Yang *et al.* used a chemically exfoliated (ce) method to synthesize ce- $MoS_2$  nanosheets and studied their antibacterial activity [82]. They found that ce- $MoS_2$  nanosheets could dramatically reduce the viability of *E. coli* in a short time, and show concentration- and time-dependent GSH oxidation capacity. Therefore, the antibacterial activity of ce- $MoS_2$  nanosheets is attributed to ROS-independent oxidative stress. In addition, Mrinmoy's group revealed that the surface charge and hydrophobicity of ce- $MoS_2$  nanosheets can be altered by modifying with different thiol ligands (**Figure 3D**), and such functionalized ce- $MoS_2$  nanosheets can be endowed with remarkable antibacterial effect by ROS-independent oxidative stress and depolarization of the bacterial membrane [83]. Intriguingly, ce- $MoS_2$  nanosheets showed higher GSH oxidizability than functionalized  $MoS_2$  nanosheets (**Figure 3E**), which is responsible for the ROS-independent oxidative stress generated by ce- $MoS_2$  nanosheets. What's more, they also found that the surface functionalization can affect antibacterial pathway, and non-functionalized  $MoS_2$  nanosheets against bacteria mainly through ROS-induced oxidative stress, while functionalized  $MoS_2$  nanosheets kill bacterial through both ROS-independent oxidative stress and bacterial

membrane depolarization. Although vast research has substantiated the striking germicidal ability of graphene oxide (GO) and MoS<sub>2</sub> nanosheets, the relevant study of 2D nanosheet-coated films for biomedical devices is still rare. Based on this, Kim *et al.* prepared a GO-MoS<sub>2</sub> nanocomposite film with outstanding antibacterial effects [84]. They found that GO-MoS<sub>2</sub> nanofilms have higher ROS-independent oxidation capacity, and its antibacterial effect is mostly achieved through ROS-independent oxidative stress. Furthermore, Navale *et al.* also reported that the reduced graphene oxide-tungsten disulphide (rGO-WS<sub>2</sub>) nanosheets had a significant bacterial inhibitory effect compared to pure WS<sub>2</sub> or rGO. They observed that rGO-WS<sub>2</sub> composites have the highest oxidation capacity towards GSH, and proposed that the GSH membrane mechanism stress may originate

from the direct contact with nanosheets, and ROS-independent oxidation stress was the major antibacterial mechanism [85].

### 2.3 Photo-Induced Antibacterial Effects

It is well-known that light-induced antibacterial mainly utilized photoconversion of excited photoactive fluorophores in photosensitizer, photothermal agents and other semiconductor nanomaterials into heat or ROS for PTT, PCT or PDT [37, 38, 86, 87]. Therefore, in recent years, these photo-induced antibacterial methods have been considered as a promising antibacterial mechanism due to their peculiar merits such as noninvasiveness, targeted selective treatment, and minimized side effects.

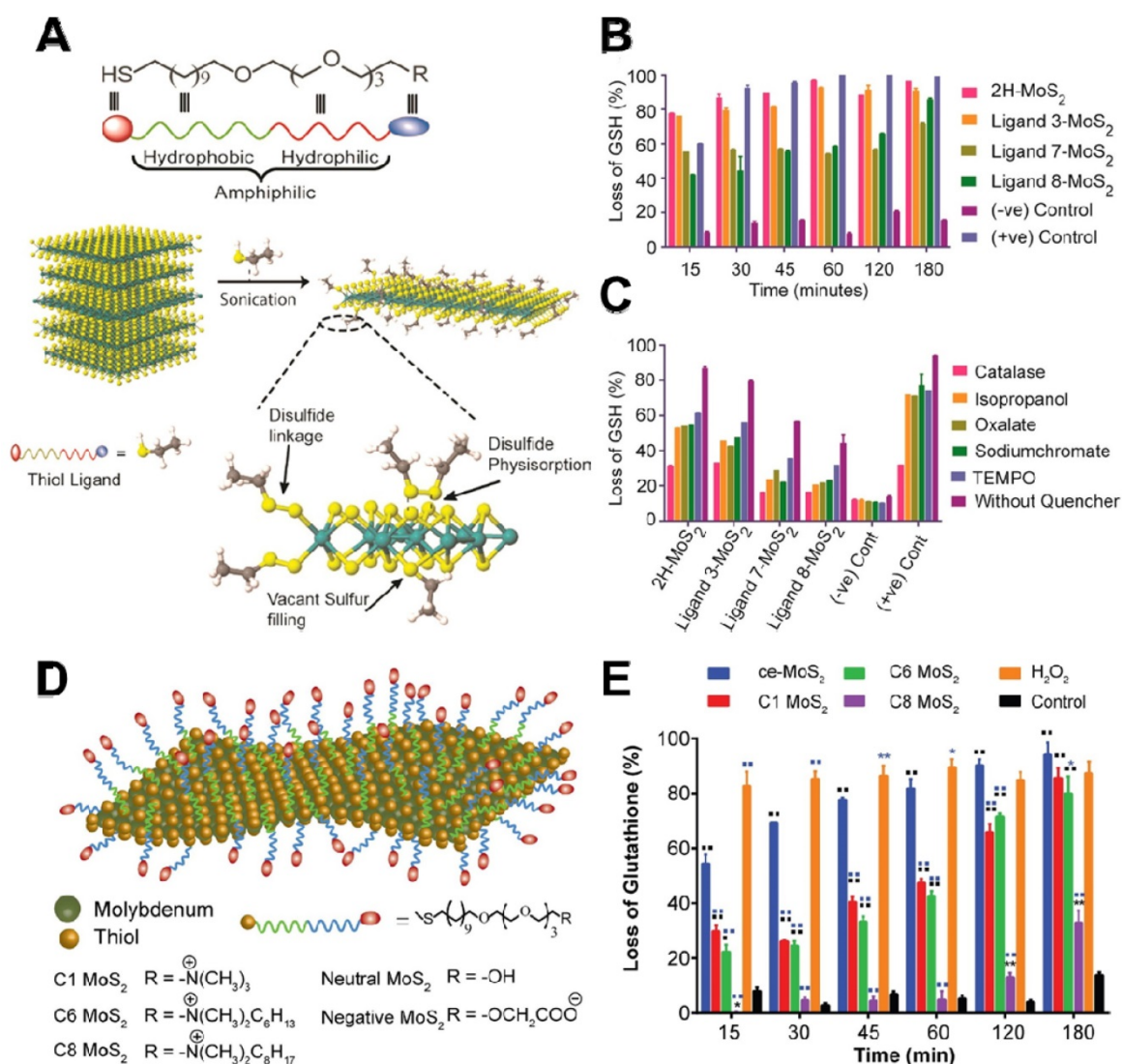


**Figure 3.** (A) Scheme for the exfoliation of 2H-MoS<sub>2</sub> with amphiphilic ligand. (B) Abiotic oxidative stress estimation by Ellman's assay with 0.4 mM glutathione. (C) Estimation of the type of ROS species in the presence of different ROS scavengers. Reproduced with permission from [74], copyright 2018 American Chemical Society. (D) Schematic representation of functionalized ce-MoS<sub>2</sub> with thiol ligands of varied charge and hydrophobicity. (E) Abiotic glutathione oxidation assay for quantification of oxidative stress generated. Reproduced with permission from [83], copyright 2016 American Chemical Society.

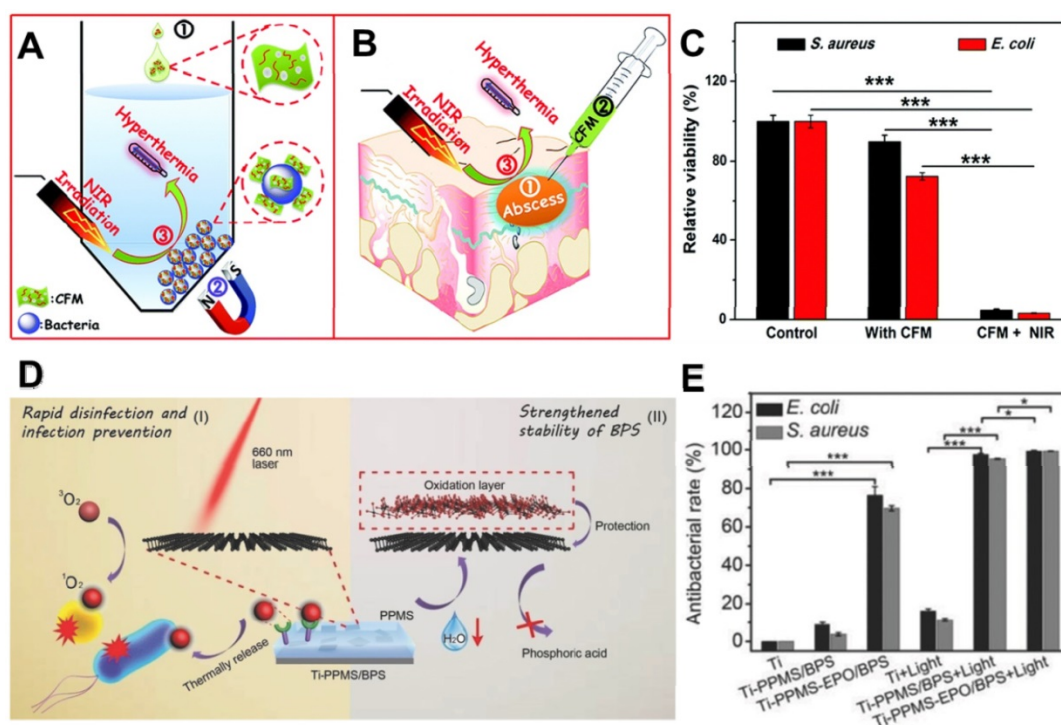


**Figure 4.** (A) *In vitro* conjugating and photothermal killing of bacteria, (B) and *in vivo* photothermal treatment of a focal infection using chitosan functionalized magnetic MoS<sub>2</sub>. (C) Antibacterial activity of the chitosan functionalized magnetic MoS<sub>2</sub> nanocomposites with or without NIR laser irradiation for *S. aureus* and *E. coli*. Reproduced with permission from [95], copyright 2016 Royal Society of Chemistry. (D) Schematic that shows the PPMS/BPS inactivating bacteria through generating <sup>1</sup>O<sub>2</sub> in the presence and absence of light, and the stability of BPS can be improved by PPMS. (E) Antibacterial performance *in vitro*. Reproduced with permission from [122], copyright 2018 WILEY-VCH Verlag GmbH & Co. KGaA, Weinheim.

### 2.3.1 Photothermal Antibacterial

Photothermal antibacterial is an important antibacterial approach, which refers to the efficient generation of heat by nanomaterials under the irradiation of light at a proper power density to kill bacteria [37]. Near-infrared (NIR) photothermal nanoagents are preferred for antibacterial due to their deep biological tissue penetration capability and minimal damage to healthy tissues. In recent years, researchers have demonstrated that various 2D NBG display remarkable photothermal antibacterial ability owing to their strong photothermal conversion efficiencies, such as MoS<sub>2</sub> [88], metal-based nanomaterials [89], Sb<sub>2</sub>Se<sub>3</sub> [90], LDH-based compounds [91], and BP nanosheets [92]. Among them, MoS<sub>2</sub> nanosheets have attracted considerable attention as typical photothermal antibacterial agents due to their high NIR photothermal conversion efficiency [93, 94]. Based on it, Zhang *et al.* prepared versatile chitosan functionalized magnetic MoS<sub>2</sub> as bacterial cross-linking and photothermal agents for *in vitro* photothermal sterilization (Figure 4A), and *in vivo* focal infection treatment (Figure 4B) [95]. The nano-agent could cause rapid aggregation and bacteria arrest in both *S. aureus* and *E. coli*, thereby enhancing the photothermal antibacterial effect. Under NIR irradiation, the temperature of the

nano-agent solution (100 µg mL<sup>-1</sup>) could reach around 45 °C within 10 min, and the bacteria survival rate decreased over 90% (Figure 4C). Besides, this nano-agent nanoplatform could also effectively convert NIR light into localized heat for treating *in vivo* focal infection. More recently, Ma *et al.* developed a core-shell gold nanorod@layered double hydroxide (GNR@LDH) nanomaterial for enlarging PTT antibacterial and tumor therapy [91]. They found that the thermal energy conversion of GNR@LDH can be significantly enhanced after 808 nm laser irradiation, which is mainly due to the production of electron deficiency on gold surface. As shown above, the burgeoning photothermal nanomaterials with strong NIR light absorbance/convert capacity revealed that the generated heat can not only kill drug-resistant bacteria but also inhibit the formation of biofilm. Therefore, 2D NBG based PTT is deemed as a safe and efficient strategy to combat bacterial infections.

### 2.3.2 Photocatalytic/Photodynamic Antibacterial

It is well-known that the photo-induced production of ROS could cause distinct oxidative stress to bacteria. Generally, the photo-mediated ROS generation mainly includes two ways: photocatalytic and photodynamic process. Photocatalytic antibacterial refers to light-induced bacteria inactivation, which depends on the efficient

generation of highly oxidative ROS by the separation of holes ( $h^+$ ) and electrons ( $e^-$ ) in the valence band (VB) and conduction band (CB) under light irradiation [96]. For many 2D NBG, they can generate photo-induced ROS to attack bacteria under ultra violet (UV) or visible light illumination. Normally, the photocatalytic disinfection process mainly includes three steps: (i) 2D NBG with large surface area can bind to bacterial surface, which provide more active sites for catalytic reactions; (ii) the formation of a photo-induced charge-separated state; (iii) the interactions of activated charge-separated centers and neighboring oxygen and water molecules can produce ROS [97]. Bismuth oxybromide (BiOBr) nanosheets, as a major 2D layered semiconductor, have attracted tremendous attention owing to its outstanding physicochemical prosperities and excellent visible light photocatalytic activity [98]. To further efficiently harvest solar energy, Wong's group fabricated bismuth oxybromide (BiOBr) nanosheets and doped with boron (B), where they further found that B-BiOBr nanosheets could effectively enhance photocatalytic bacteria inactivation through photogenerated  $h^+$  mediated mechanism [99]. Firstly, light motivated BiOBr to generate  $e^-$  in its CB, and leave  $h^+$  in its VB. Then, B as a good  $e^-$  acceptor could promote an extra  $e^-$  from VB to CB and cause abundant  $h^+$  gathering in VB, which could enhance the  $e^-/h^+$  pair separation efficiency of BiOBr. Finally, the amount of  $h^+$  with higher oxidative ability could directly oxidize bacteria, leading to photocatalytic bacteria inactivation. They also found that B-BiOBr nanosheets show apparent photocatalytic disinfection activity towards *E. coli*, and the increased content of B dopant could dramatically enhance the antibacterial properties. Moreover, Wu *et al.* demonstrated that self-doped  $Bi^{5+}$  or  $Bi_2O_4$  decorated BiOBr nanosheets display a much higher photocatalytic inactivation activity than pure BiOBr nanosheets [100, 101]. Recently,  $g-C_3N_4$  has been a rising star in the field of photocatalyst disinfection as it could harvest substantial visible light for achieving highly efficient photocatalytic performance [102-104]. For example, Huang *et al.* for the first time revealed that  $g-C_3N_4$  nanosheets exhibited excellent photocatalytic bactericidal effects toward *E. coli* under visible light irradiation, without any bacterial regrowth [105]. Several cumulative studies have documented that exfoliating the bulk  $g-C_3N_4$  into  $g-C_3N_4$  nanosheets could improve the photocatalytic performance. To this end, Zhao *et al.* fabricated single layer  $g-C_3N_4$  nanosheets by thermal etching and ultrasonic exfoliation. They found that a total of  $2 \times 10^7$  CFU  $mL^{-1}$  of *E. coli* could be destroyed completely within 4 h after incubated with single layer  $g-C_3N_4$  nanosheets

under visible light irradiation, which is much higher than bulk  $g-C_3N_4$  nanosheets [106]. Besides, some other 2D NBG, such as  $MoS_2$ ,  $TiO_2$ ,  $Bi_2WO_6$ ,  $ZnO$ , as well as metal-free nanomaterials, also exhibited outstanding photocatalytic antibacterial activity [97, 104, 105, 107-109]. To further improve the photocatalytic antibacterial activity, the integration of various photocatalysts or co-catalysts, such as  $Ag-ZnO/g-C_3N_4$  [110],  $g-C_3N_4$  NS/RGO/CA [111],  $V_2O_5/BiVO_4$  [112], graphene/ $g-C_3N_4$  [113],  $TiO_2/g-C_3N_4$  [114],  $TiO_2-Bi_2WO_6$  [108], and  $Bi_2MoO_6/g-C_3N_4$  [115], has been widely investigated as an effective modification strategy. Although photocatalytic disinfection represents one of the most promising disinfection mechanisms, important issues such as catalyst immobilization, recycling methods, photocatalytic reactor design as well as optimization of disinfection parameters of 2D NBG need to be addressed for future practical applications.

In addition to above photocatalytic-induced bacteria elimination, PDT as another light-induced ROS generating modality for minimally invasive antibacterial has also been reported [86]. It mainly employs appropriate excitation light and oxygen molecules as exogenous stimuli to selectively activate photosensitizers at the targeted region, producing various cytotoxic ROS like  $^1O_2$  and  $\bullet OH$  to effectively damage the bacterial membrane, nucleic acids, proteins, and even DNA. Additionally, PDT can also eliminate biofilms by degrading their excretive products [116]. Notably, PDT has several advantages over other conventional antibacterial strategies owing to its noninvasive property, massive loading capability, and fast healing process. PDT can be carried out through two paths: type I and type II. Under light irradiation, photosensitizers migrate from ground state to single excited state, and then reach to triple excited state [117, 118]. For type I, the triple excited-state photosensitizers directly react with the biological substrates to generate  $\bullet OH$  or  $\bullet O_2$  through electron transfer, and this process not only break the structural integrity of the bacterial membranes but also enhance ionic permeability of bacteria cell membrane [119]. For type II, triple excited-state photosensitizers could directly transfer energy with the surrounding  $^3O_2$  to produce cytotoxic  $^1O_2$ , and the  $^1O_2$  can effectively kill bacteria by causing oxidative damages to unsaturated lipids, enzymes, DNA, peptides, and other cellular components [120]. Currently, various 2D nanomaterials such as  $MoS_2$  nanosheets, BP nanosheets, fullerenes, graphene,  $ZnO$ , and  $TiO_2$ , show inherent photosensitivity, and they have been widely explored for PDT through generating ROS upon light irradiation [121]. Recently, Tan *et al.* designed a novel PDT antibacterial system

based on the integration of BP nanosheets and poly (4-pyridonemethylstyrene) (PPMS), achieving the storage and release of  $^1\text{O}_2$  for rapid disinfection and infection prevention (**Figure 4D**) [122]. Intriguingly, BP nanosheets were used as a photosensitizer to generate  $^1\text{O}_2$  under light irradiation. Simultaneously, the PPMS were composited with the BP nanosheets to store singlet  $^1\text{O}_2$ , and the  $^1\text{O}_2$  was released by thermal decomposition. They found that this system showed an excellent PDT antibacterial effect with or without light irradiation (**Figure 4E**). Therefore, 2D-based nano-photosensitizers as light-triggered bactericides show great potential for PDT antibacterial.

## 2.4 Controlled Drug/Metallic Ions Release for Antibacterial

The ability of controllable release drug/metallic ions is widely accepted as an important antibacterial process of 2D NBG [123]. Due to their large surface area, 2D NBG can act as nanocarriers with controlled release of antibacterial agents under particular stimuli [124]. Currently, the release of antibacterial agents mainly include either converting unstable organosulfur compounds into stable inorganic sulfur compounds [125] or loading traditional antibiotics (cefazolin [126], tetracycline hydrochloride [127], and curcumin *etc.* [128]), noble metallic ions (such as Ag ions [129-131]) and molecular donor (NO [132],  $\text{H}_2\text{S}$  donor [133]) into 2D NBG surface. Ultimately, released drugs or metallic ions on the surface of 2D NBG can inactivate the bacteria through interfering essential cellular components such as cell membrane integrity, respiration, and adenosine triphosphate (ATP) production. Recently, Gao's group proposed a novel nano-conversion strategy for enhancing antibacterial activity through converting natural

organosulfur compounds into nano-iron sulfides (FeS), where the enhanced antibacterial effect benefited from cysteine-nFeS (Cys-nFeS) with enzyme-like activity could effectively increase the release of bactericidal polysulfanes (**Figure 5A**) [134]. The antibacterial results also showed that Cys-nFeS not only display a broad antibacterial activity against *Pseudomonas aeruginosa* (*P. aeruginosa*), *E. coli*, and *S. aureus*, but also could effectively inhibit the formation of biofilms and accelerate infected-wound healing. Moreover, it is well-known that Ag ions can combine with proteins, nucleic acid, and enzymes in microorganisms, causing a serious deformation of the bacteria membrane to ultimately kill bacteria [135]. To this end, Cao *et al.* constructed an efficient and benign antibacterial depot (PDDA-Ag<sup>+</sup>-Cys-MoS<sub>2</sub>) with Cys-modified MoS<sub>2</sub> loaded with minimum Ag ions and coated with cationic polyelectrolyte (**Figure 5B**) [136]. This system displayed remarkable antibacterial activity toward both *E. coli* and *S. aureus* compared with an equivalent amount of silver nitrate, due to its enhancing accessibility of released Ag ions to the bacterial wall (**Figure 5C, D**). In addition, antibiotic-loaded MoS<sub>2</sub> nanosheets and MoS<sub>2</sub>-modified curcumin nanostructures could effectively release antibacterial agents against multidrug-resistant bacteria [127, 128]. To enhance the antibacterial activity of this disinfection process, high concentrations of 2D NBG nanocarriers are necessary. However, due to the toxicity of metallic ions, it is important to regulate the concentration of metal ions in an acceptable range. Therefore, the effective removal of metal ions and 2D NBG from *in vivo* also requires a deeper investigation in the future.

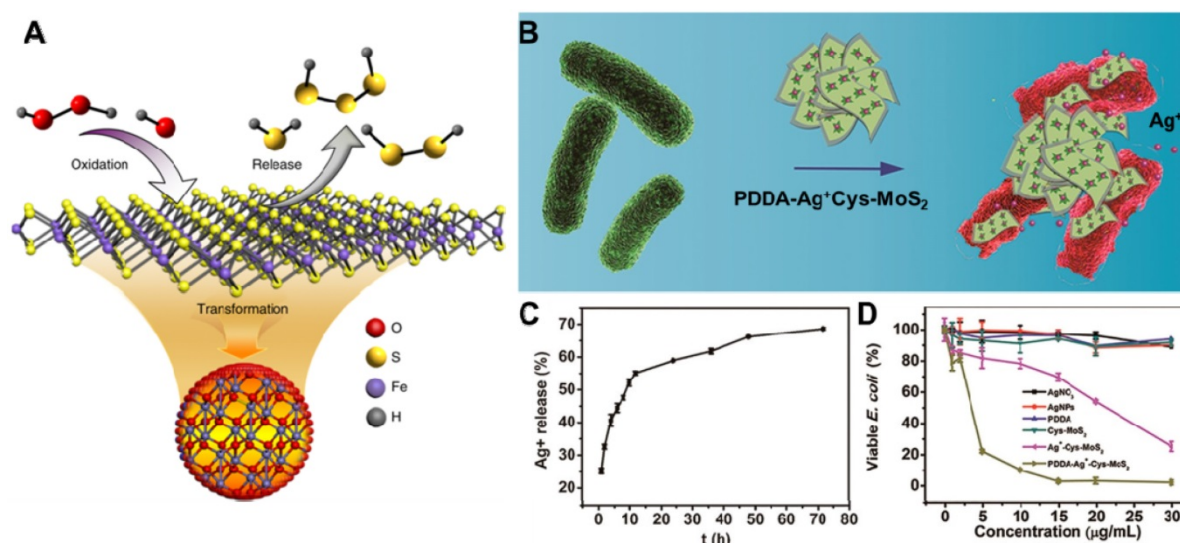


**Figure 5.** (A) Scheme of polysulfane release from nFeS. Reproduced with permission from [134], copyright 2018 Nature Publishing Group. (B) The PDDA-Ag<sup>+</sup>-Cys-MoS<sub>2</sub> depot for antibacterial applications. (C) Cumulative silver ion release profiles from PDDA-Ag<sup>+</sup>-Cys-MoS<sub>2</sub> samples. (D) Viability analyses of *E. coli*. Reproduced with permission from [136], copyright 2017 American Chemical Society.

## 2.5 Synergistic Antibacterial

In the previous sections, we have detailed introduced the typical antibacterial mechanisms of 2D NBG based on their intrinsic antibacterial properties. However, the complexity, diversity, and multidrug resistance of bacteria seriously impede the development potential of 2D NBG for disinfection. The antibacterial mechanisms mentioned above also suffer from their respective shortcomings, which limit their further antibacterial application. For example, the mechanism of physical contact destruction could only kill the bacteria attached on the surface of 2D NBG, and the long-term antibacterial efficiency could significantly decrease with the degradation of nanomaterials. For the oxidative stress antibacterial mechanism, the antibacterial effects mainly depend on the specific surface area, conductivity, and size of the 2D NBG. Although light-induced antibacterial mechanisms were deemed as one of the generally accepted efficient antibacterial strategies, the targeted killing bacteria ability, the hypoxia infected areas, and the photocatalytic efficiency are still prominent factors limited their antibacterial performances. In addition, for the release of metallic ions or drugs, the overuse may also bring serious toxicity to normal tissues. Thus, current study trend has gradually converted from the concentration on mono-mode antibacterial to 2D NBG-mediated multi-mode synergistic antibacterial for enhanced antibacterial effect. Currently, 2D NBG was often employed as nanocarriers to deliver other antibacterial agents (such as drugs, metallic ions, gas donor, and antibacterial polymers) into infected areas, which attain striking synergistic antibacterial effects that are stronger than that of any antibacterial strategy alone. Here, we summarize several common 2D NBG-mediated synergistic antibacterial methods: (i) synergy of PTT with PDT [137-139]; (ii) synergy of PTT with metallic ions release (Ag, Au, etc.); (iii) synergy of chemotherapy with PTT [140]; (iv) synergy of PTT with oxidative stress [79]; (v) synergy of PTT with catalytic [139, 141-144]; (vi) and tri-modal synergistic antibacterial [145, 146]. At the same time, the synergetic antibacterial mechanism and application are detailedly discussed.

In recent years, PTT antibacterial has been widely accepted by researchers. The generation of heat by PTT can not only directly destroy the bacteria but also accelerate blood flow so as to effectively improve the intracellular generation of ROS for enhanced PDT. To this end, Wu's group synthesized a chitosan-assisted MoS<sub>2</sub> (CS@MoS<sub>2</sub>) hybrid with a coating on the surface of Ti material, which showed rapid *in situ* antibacterial effect [147]. They demonstrated that the synergistic effects of PDT and

PTT actions of CS@ MoS<sub>2</sub>-Ti under dual lights irradiation (660 nm visible light and 808 nm NIR) could significantly enhance the antibacterial effect towards *E. coli* and *S. aureus* (Figure 6A, B). Besides, Wu's group prepared hybrid nanosheets based on g-C<sub>3</sub>N<sub>4</sub>-Zn<sup>2+</sup>@graphene oxide for rapid sterilization and accelerated wound healing under dual light irradiation [139]. They found that the hybrid nanosheets could achieve an antibacterial ratio over 99.1% within a short time due to the synergistic effects of PDT and PTT. In addition, Wang's group used polydopamine (PDA), MoS<sub>2</sub> nanosheets and silver nanoparticles to form MoS<sub>2</sub>@PDA-Ag nanosheets (MPA) as a novel dual antibacterial nanoagent [148]. On the one hand, under NIR irradiation, the MPA nanosheets could generate heat, and directly damage the bacterial biofilm and the bacterial membrane. On the other hand, PTT also accelerates Ag ions release, enhancing the antibacterial efficacy of Ag ions. Therefore, the therapy strategy of combining PTT and metallic ions release is helpful for addressing the lower single antibacterial effect. In addition, Yuan *et al.* fabricated a functional MoS<sub>2</sub>/PDA-arginine-glycine-aspartic acid (RGD) to inhibit bacterial infection *in situ* and improve osseointegration [79]. They found that NIR-induced hyperthermia of MoS<sub>2</sub>/PDA-RGD samples could efficiently increase GSH oxidation. Besides, the intrinsic ROS-independent oxidative stress of MoS<sub>2</sub> nanosheets could also destroy the integrity of the bacterial membrane, finally significantly killing bacteria. After NIR irradiation, the antibacterial efficiency of MoS<sub>2</sub>/PDA-RGD reached 96.6% for *S. aureus* and 97.8% for *E. coli*, which is ascribed to the synergism between PTT and oxidative stress. Some antibiotic drugs, such as penicillin (pen), curcumin and lysozyme can be controllably released from 2D NBG surface. Based on which, Zhang *et al.* constructed an antibacterial nanomaterial through a polyphenol-assisted exfoliation strategy to exfoliate MoS<sub>2</sub> nanosheets and loading antibiotic drugs pen onto MoS<sub>2</sub> nanosheets surface (Figure 6C), which exhibited robust antibacterial effect *via* a synergetic of NIR-driven PTT and Pen-induced chemotherapy (Figure 6D) [140]. Furthermore, our previous study demonstrated that polyethylene glycol functionalized MoS<sub>2</sub> nanoflowers (PEG-MoS<sub>2</sub> NFs) with peroxidase-like catalytic activity could be used for treating *in vivo* wound infection, which could convert low dosage clinical H<sub>2</sub>O<sub>2</sub> into more toxic •OH. Together with the NIR photothermal ability of MoS<sub>2</sub>, it could realize synergetic PTT/catalytic antibacterial (Figure 7A, B) [143]. Intriguingly, PEG-MoS<sub>2</sub> NFs exhibited a time-dependent and hyperthermia-enhanced oxidation behavior, and after incubation

with PEG-MoS<sub>2</sub> NFs (80 µg mL<sup>-1</sup>) for 6 h the statistical loss of GSH can reach to 73.4% (Figure 7C). Furthermore, compared to the water bath group at 50 °C, the hyperthermia induced by PEG-MoS<sub>2</sub> NFs showed a much higher GSH oxidation level (Figure 7D). Recently, Qu's groups firstly developed a nanozyme with abundant defects that have enhancing bacterial capturing abilities and efficient enzyme catalysis antibacterial effects [144]. Briefly, the nanozyme with rough surface not only can efficiently trap bacteria, but also the defect-rich edges exhibit higher intrinsic peroxidase-like activity than pristine structures, which generate amounts of toxic •OH around the bacteria and exhibit considerable bacterial inhibition effect. Aside from the above mentioned dual-mode synergistic antibacterial, Yin *et al.* designed a tri-modal synergistic antibacterial agent (MoO<sub>3-x</sub>-Ag) for cleaning the bacterial contaminated water environment [145]. They found that the as-designed MoO<sub>3-x</sub>-Ag killed pathogenic bacteria mainly through (i) photothermal effect of MoO<sub>3-x</sub> nanosheets upon NIR irradiation; (ii) NIR light excitation of MoO<sub>3-x</sub>-Ag trigger the release of Ag ions; and (iii) photocatalytic reaction. Moreover, Roy *et al.*

prepared chitosan exfoliated MoS<sub>2</sub> nanosheets (CS-MoS<sub>2</sub>) and investigated their intrinsic antibacterial mechanism [146]. They found that the CS-MoS<sub>2</sub> nanosheets could kill bacteria through a synergistic effect of ROS-dependent oxidative stress, physical contact caused membrane damage and metabolic inactivation.

## 2.6 Effect of Physicochemical Properties on the Antibacterial of 2D NBG

It is well-known that the antibacterial effect of 2D nanomaterials can be significantly influenced by their intrinsic physicochemical properties, such as size, shape, number of layers, phase structure, and surface functionalization. Firstly, the size of 2D nanomaterials is a key factor in governing the antibacterial effect because size can strongly influence the dispersibility and adsorption ability, which are crucial to the interactions between 2D nanomaterials and bacteria. For instance, a relatively smaller size of Ag nanoparticles can increase the interaction with bacteria and exhibit higher antibacterial activity [149-151]. Then, the shapes of 2D nanomaterials are also found to largely influence the germicidal ability.

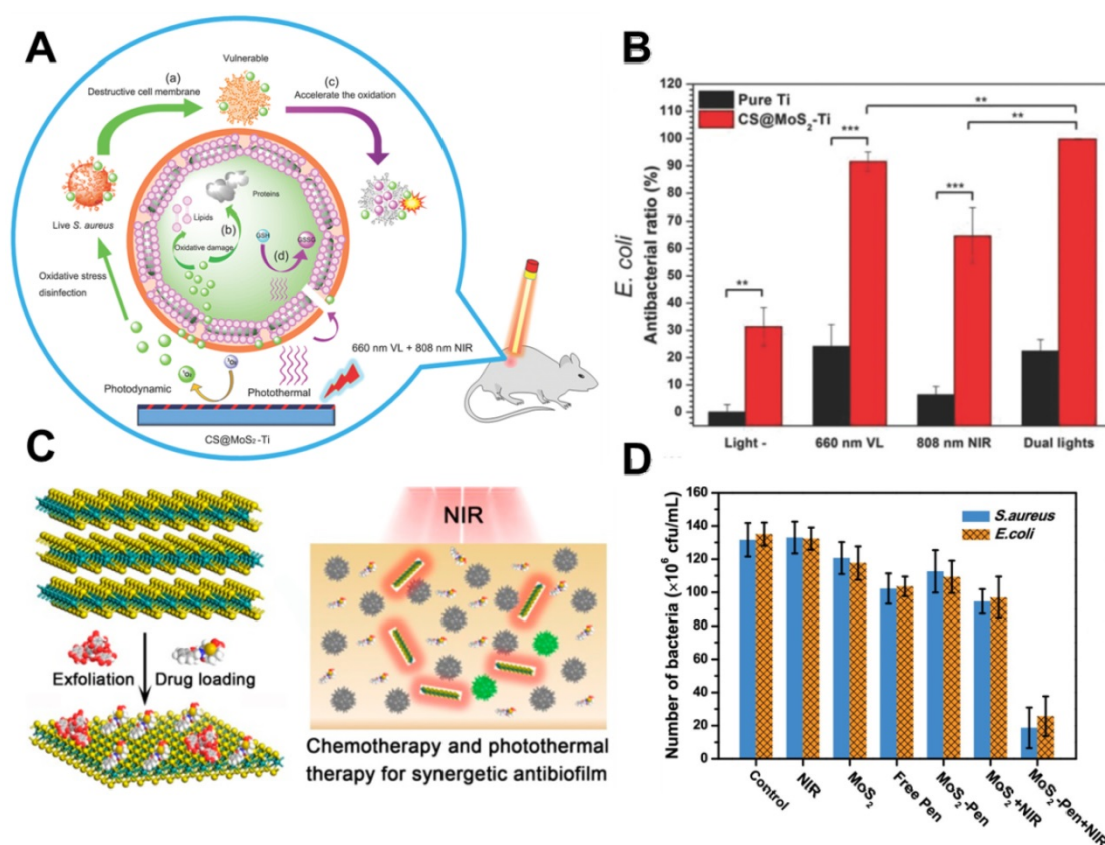


**Figure 6.** (A) Schematic illustration of CS@MoS<sub>2</sub> hybrid coating constructed on the surface of Ti material for synergistic photodynamic and photothermal antibacterial action under the dual lights irradiation. (B) The antibacterial activity *E. coli* and *S. aureus* of pure Ti and CS@MoS<sub>2</sub>-Ti under the conditions of darkness (light) and after exposing to 660 nm visible light; 808 nm NIR; dual lights for 10 min. Reproduced with permission from [137], copyright 2018 WILEY-VCH Verlag GmbH & Co. KGaA, Weinheim. (C) The Pen-loaded MoS<sub>2</sub> nanosheets exhibit outstanding antibiofilm activity via synergistic chemotherapy and photothermal therapy. (D) Number of *S. aureus* and *E. coli* in the presence of different antibacterial agents: control, NIR light, MoS<sub>2</sub> nanosheets, free Pen, MoS<sub>2</sub>-Pen nanosheets, MoS<sub>2</sub> nanosheets with NIR light, and MoS<sub>2</sub>-Pen nanosheets with NIR light. Reproduced with permission from [140], copyright 2018 American Chemical Society.

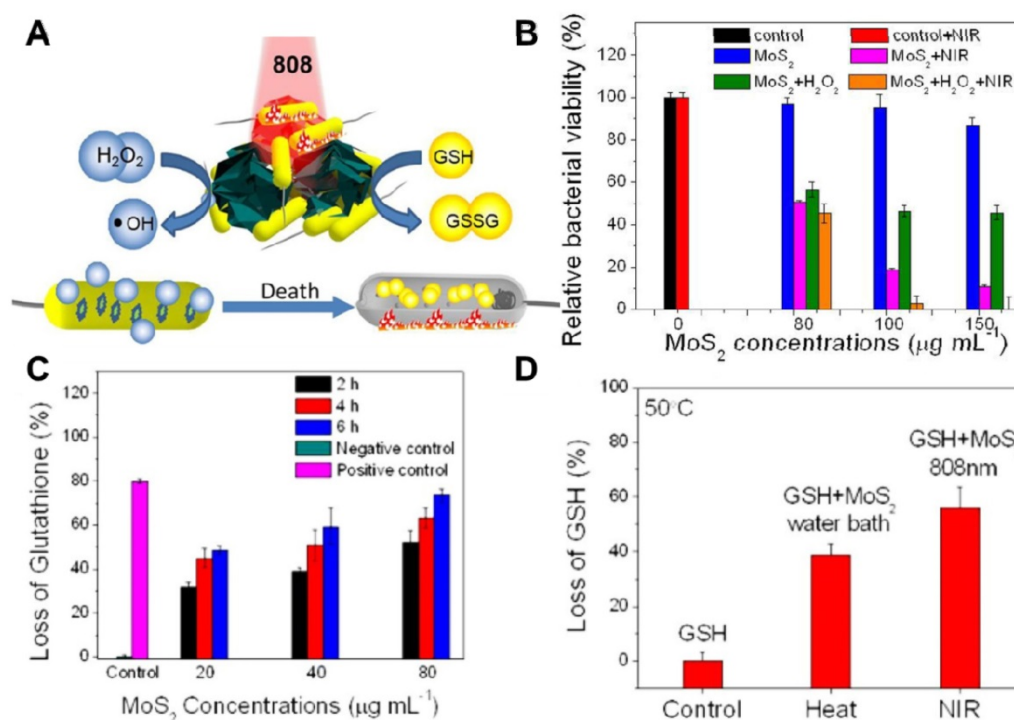


**Figure 7.** (A) Schematic illustration of PEG-MoS<sub>2</sub> for peroxidase catalyst and photothermal synergistic antibacterial. (B) Relative bacterial viability of *Ampr E. coli* incubated with different concentrations PEG-MoS<sub>2</sub> NFs with or without H<sub>2</sub>O<sub>2</sub> (100 μM) under 808 nm laser irradiation. (C) Loss of GSH plot after incubation with PEG-MoS<sub>2</sub> at different time intervals. (D) Loss of GSH plots heated by water bath and NIR 808 nm irradiation, respectively, for 20 min at 50°C. Reproduced with permission from [143], copyright 2018 American Chemical Society.

It was revealed that the shapes of 2D nanomaterials would affect its interaction strength with the bacterial membrane, which greatly influences electron-transfer-based oxidative stress antibacterial activities. For example, Ananth *et al.* prepared spherical and sheet-like ruthenium oxide (RuO<sub>2</sub>) nanomaterials, and their shape-dependent anti-bacterial activities were carried out. Results showed that RuO<sub>2</sub> nanosheets displayed higher antibacterial activity compared with RuO<sub>2</sub> nanospheres [152]. Moreover, the numbers of 2D NBG layers also influence antibacterial performance. Normally, thinner nanomaterials can easily damage the bacterial cell wall, and causing outstanding antibacterial effect. For instance, Sun *et al.* used N,N'-dimethylpropyleneurea as a new exfoliating solvent to effectively produce higher crystalline and free defects of BP nanosheets, and found that exfoliated BP nanosheets exhibited thickness-dependent photothermal antibacterial effects [153]. In addition, the phase structure of layered TMDCs nanomaterial also affects their antibacterial activity. In general, due to the differences in coordination geometry between metal and chalcogen atoms, TMDCs mainly include the 1T phase and 2H phase [154]. The 1T phase structure of TMDCs with metallic character can be used in cell destruction using NIR PTT effect [88], while the 2H phase structure with semiconducting and photolumi-

nescence property can be utilized in visible light-induced water disinfection [97]. According to research findings, the antibacterial capacity of exfoliated 1T-MoS<sub>2</sub> nanosheets is higher than the annealed exfoliated 2H-MoS<sub>2</sub> nanosheets, which is attributed to the higher electron conductivity in 1T-MoS<sub>2</sub> nanosheets [75]. Finally, the surface functionalization also affects the antibacterial performance of 2D NBG through changing their surface charge [155]. For instance, 2D nanomaterials modified with positively charged groups could efficiently attach to the negatively charged bacterial membrane, which presents higher antibacterial activities [74].

### 3. 2D NBG Antibacterial Nanomaterials

In the past few years, there have been large amounts of research that concentrate on 2D NBG and their bactericidal applications. Taking inspiration from the excellent antibacterial performances of graphene, the potential antibacterial applications of 2D NBG, such as transition-metal dichalcogenides/oxides (TMDC/Os), metal-based nanocompounds, C<sub>3</sub>N<sub>4</sub>, BP, MXenes and other burgeoning 2D NBG materials have also been researched. Here, a summary of the recent progress of the 2D NBG antibacterial applications is in **Table 1**, and the detailed introduction is given below.

**Table 1.** A summary of 2D NBG for antibacterial application

Category	Nanomaterials	Morphology, size & surface modification	Type of Bacteria	Antibacterial Mechanism & effect	Refs.	
TMDC/Os	CS@MoS <sub>2</sub>	Monolayer NSs, Chitosan modified	<i>E. coli</i> , <i>S. aureus</i>	PDT & PTT cause the disruption of membrane integrity & leakage of cytoplasmic components; >99%	[41, 137, 156]	
	Magnetic MoS <sub>2</sub>	NSs, Chitosan functionalized	<i>E. coli</i> , <i>S. aureus</i>	Enhance the conjugation of bacterial & PTT; >90%	[95]	
	MoS <sub>2</sub> -Pen	Monolayer NSs, 38.6±1.3 nm, Pen-loaded	<i>E. coli</i> , <i>S. aureus</i>	chemotherapy & PTT synergetic effect; kill the majority of bacterial	[140]	
	PEG-MoS <sub>2</sub>	334 nm NFs, PEG modified	<i>E. coli</i> , <i>B. subtilis</i>	Peroxidase-like catalysis and PTT synergetic antibacterial; up to 97%	[143]	
	MoS <sub>2</sub> -BNN6	Single-layer NSs, 50~80 nm, α-cyclodextrin modified	<i>Amp<sup>r</sup> E. coli</i> , <i>E. faecalis</i>	PTT & NO-enhanced free radical generation synergetic antibacterial, highly effective bacterial inactivation (>97.2%)	[157]	
	pyramid MoS <sub>2</sub> @Ag	Triangles, 5 to 10 μm	<i>E. coli</i>	Photocatalytic generate ROS; more than 99.99%	[158]	
	MoSe <sub>2</sub>	100 nm NSs, without modified	<i>E. coli</i> , <i>B. subtilis</i>	Peroxidase-like activity could catalyze H <sub>2</sub> O <sub>2</sub> into •OH for antibacterial; ~100%	[159]	
	MoO <sub>3</sub>	plate-like structures	<i>E. coli</i> , <i>S. aureus</i> , <i>E. faecalis</i> , <i>B. subtilis</i>	Disruption of the bacterial cell wall; Effective	[63]	
	MoO <sub>3-x</sub> -Ag	Around 300 nm NSs, without modified	<i>E. coli</i> , <i>S. aureus</i>	PTT, Ag+ release & photocatalytic synergetic effect; 99.2% of <i>E. coli</i> and 97.0% of <i>S. aureus</i> are killed	[145]	
	WS <sub>2</sub>	2~3 layers 200 nm NSs	<i>E. coli</i> , <i>S. aureus</i>	ROS generating & damage the structural integrity of bacterial membrane	[65]	
Metal-based	WX <sub>2</sub> -ssDNA	65~650 nm NSs	<i>E. coli</i>	ROS-independent oxidative stress; around 82.3%	[78]	
	PDMS/WS <sub>2</sub>	Single-layer less than 1 μm nanoflowers	<i>E. coli</i>	ROS generating; more than 99.99%	[160]	
	WS <sub>2</sub>	Monolayer NSs, Ag decorated	<i>E. coli</i>	Ag enhance the photocatalytic efficiency; up to 96%	[161]	
	Pd@Ag	hexagonal plate-like shapes, 85 nm	<i>E. coli</i> , <i>S. aureus</i>	the synergetic effect of PTT & NIR-triggered Ag <sup>+</sup> release; almost 100% bacteria	[162]	
	Ag/CS@MnO <sub>2</sub> -TiO <sub>2</sub>	Chitosan functionalized	<i>E. coli</i> , <i>S. aureus</i>	PTT & Ag ions release synergetic effect; up to 99.00%	[163]	
	TiO <sub>2</sub>	Sizes controllable NSs, Amine modified	<i>E. coli</i>	Photocatalytic antibacterial activity; around 89%	[164]	
	MoS <sub>2</sub> -TiO <sub>2</sub>	Sheet-like morphology	<i>E. coli</i> , <i>S. aureus</i>	Effective	[165]	
	g-C <sub>3</sub> N <sub>4</sub>	Plane structural, etching with HCl	<i>E. coli</i>	Photocatalytic & self-cleaning; reach 100%	[166]	
	g-C <sub>3</sub> N <sub>4</sub> -Au	irregular nanosheets, about 200 nm, 1-pyrenebutanoic acid modified	<i>E. coli</i>	light-triggered ROS generation; Effective	[167]	
	Bi <sub>2</sub> MoO <sub>6</sub> /g-C <sub>3</sub> N <sub>4</sub>	Plane structural	<i>E. coli</i>	PCT antibacterial; significantly effect	[115]	
Nitride-based	Ag@g-C <sub>3</sub> N <sub>4</sub>	Ultrathin NSs, 20~40 nm	<i>E. coli</i> , <i>S. aureus</i> & <i>P. aeruginosa</i>	photocatalytic generated ROS; Effective	[168, 169]	
	Ag/PDA/g-C <sub>3</sub> N <sub>4</sub>	PDA modified	<i>E. coli</i>	Photocatalytic & Ag NPs; 99.2% of <i>E. coli</i> can be killed within 2 h	[170]	
	AgVO <sub>3</sub>	Sheet-like morphology	<i>S. aureus</i> , <i>Salmonella</i>	Photocatalytic generated ROS; killing 96.4% of bacterial within 10 min	[171]	
	QDs/g-C <sub>3</sub> N <sub>4</sub>					
	BP	215.84 ± 82.09 nm NSs	<i>E. coli</i> , <i>B. subtilis</i>	ROS-dependent oxidative stress & membrane damage; up to 91.65% and 99.69% for <i>E. coli</i> and <i>B. subtilis</i>	[77]	
	BP@silk fibroin	About 200 nm layer NSs, silk fibroin modified	<i>E. coli</i> , <i>B. subtilis</i>	NIR-mediated PTT bactericidal; eliminate most of the bacteria	[92]	
	PPMS/BPS	588 nm NSs, with modified	<i>E. coli</i> , <i>S. aureus</i>	PDT; 99.3% against <i>E. coli</i> and 99.2% against <i>S. aureus</i>	[122]	
	AuNPs/BP	Ultrathin NSs	<i>E. coli</i>	Catalytic synergistic Au; up to 94.7%	[172]	
	MXenes	Ti <sub>3</sub> C <sub>2</sub> T <sub>x</sub>	Multilayer transparent flakes, about 400 nm	<i>E. coli</i> , <i>S. aureus</i>	Physical contact lead to membrane damage; > 98%	[173]
		MoS <sub>2</sub> /MXene	About 350 nm NSs	<i>E. coli</i> , <i>S. aureus</i>	Sharp edges lead to membrane damage; >90%	[58]
Others	Ti <sub>3</sub> C <sub>2</sub> T <sub>x</sub> MXene	Single-layer NSs, few hundred nanometers	<i>E. coli</i> , <i>S. aureus</i>	Inhibit the bacterial growth and efficiently hinder the biofilm formation; > 99% growth inhibition	[174]	
	B-BiOBr	Square-like NSs	<i>E. coli</i>	Photocatalytic generated ROS; Effective	[99]	
	lyso@ZnMgAl-LDH	Flower-like morphology; Lyso modified	<i>E. coli</i> , <i>S. aureus</i>	LDH enhanced lysozyme antibacterial; fewest bacterial colonies	[175]	
	Ag-LDH	Multilayers platelet-like, 300~500 nm NSs	<i>E. coli</i> , <i>B. subtilis</i>	Kill the planktonic bacteria and biofilm inhibition; killing almost 100% of bacteria	[150]	
	Sliver/h-BN	Double layer NSs	<i>Chlorophenols arthrobacter</i>	Remarkable antibacterial activity	[176]	
	In <sub>2</sub> Se <sub>3</sub>	Multilayer NSs, about 300 nm	<i>E. coli</i>	PTT antibacterial; the bacterial inactivation percentage is 98%	[177]	
	RuO <sub>2</sub>	Spherical/ sheet like structure, PEG modified	<i>V. anguillarum</i> , <i>E. tarda</i> , <i>S. iniae</i> & <i>S. parauberis</i>	Shape dependent direct contact or oxidative stress; Effective	[152]	

**Abbreviations:** BNN6: N,N'-di-sec-butyl-N,N'-dinitroso-1,4-phenylenediamine; PEG: polyethylene glycol; TEG: tetraethylene glycol; *Pseudomonas aeruginosa*: *P. aeruginosa*; PPMS: poly (4-pyridonemethylstyrene); PDDA: polyelectrolyte poly(diallyldimethylammonium chloride); ssDNA: single-stranded DNA; PDMS: polydimethylsiloxane; PDA: polydopamine; LDH: layered double hydroxide.

### 3.1 Transition-Metal Dichalcogenides/Oxides Antibacterial Nanomaterials

In the last few decades, 2D TMDC/Os with general chemical formula of  $AB_x$  (A: transition-metal, B: chalcogen), have been studied extensively in nanotechnology field owing to their unique graphene-like properties, which are composed of a "sandwich" structure of "B-A-B" or "B-A-O" through weak Van der Waals forces [178-180]. Prototypical TMDC/Os,  $MoS_2$ ,  $MoO_2$ ,  $MoSe_2$ ,  $WO_{3-x}$ , and  $WS_2$  are the most extensively explored ones [181, 182]. For example,  $MoS_2$  nanosheets have exhibited great potential in the biomedical field due to their unique properties correlated with their 2D ultrathin atomic layer structure and high surface area [183]. Specifically, owing to its layer-dependent bandgap,  $MoS_2$  nanosheets with very broad photodetection ability can be used as a candidate for photothermal/photocatalytic antibacterial [183, 184]. Taking advantage of this feature, our groups fabricated a biocompatible 808 nm laser-mediated NO-releasing  $MoS_2$ -BNN6 nanovehicles for low-cost, rapid, and effective antibacterial (Figure 8A) [157]. We demonstrated that  $MoS_2$  nanosheets with high photothermal conversion efficiency and hyperthermia could control NO delivery and release upon 808 nm laser irradiation (Figure 8B). The synergistic effect of PTT and NO release lead to outstanding germicidal

ability toward *Amp<sup>r</sup> E. coli* (Figure 8C) and *E. faecalis* (Figure 8D). Moreover, comet assay results proved that the  $MoS_2$ -BNN6 nanovehicles presented with PTT/NO synergistic antibacterial activities could cause great DNA damage. The *in vivo* wound healing in mice demonstrated the practical applicability of this antibacterial strategy. Moreover, Liu *et al.* fabricated few-layered vertically aligned  $MoS_2$  (FLV- $MoS_2$ ) films with the ability to harvest the whole spectrum of visible light for effective photocatalytic water disinfection [97]. Due to the increased bandgap of  $MoS_2$ , from 1.3 eV (bulk material) to 1.55 eV (FLV- $MoS_2$ ), FLV- $MoS_2$  could generate considerable ROS for bacteria inactivation in water under visible light irradiation. They also found that the additional deposition of Cu or Au onto FLV- $MoS_2$  films could assist electron-hole pair separation and catalyze ROS production reactions, which allowed FLV- $MoS_2$  to realize a rapid inactivation of >99.999% bacteria within only 20 min. Similarly, Cheng *et al.* constructed a pyramid-type  $MoS_2$  (pyramid  $MoS_2$ ) on transparent glass using the chemical vapor deposition method for highly effective water disinfection under visible light irradiation [158]. They also found that the pyramid  $MoS_2$  has a smaller bandgap, which could harvest a wide spectrum of sunlight and generate more ROS for killing bacteria.

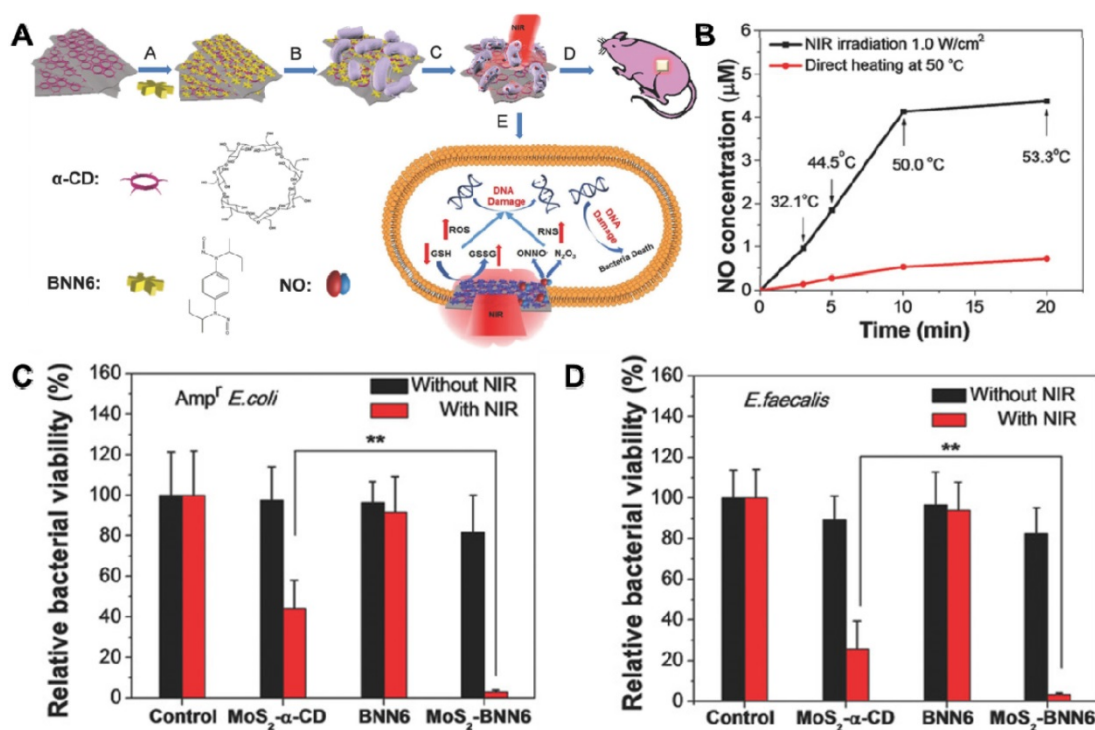


**Figure 8.** (A) Schematic illustration of  $MoS_2$ -BNN6 as NIR laser-mediated NO release nanovehicle for synergistic eliminating bacteria. (B) Effects of direct heating and 808 nm laser irradiation on NO release from  $MoS_2$ -BNN6. The corresponding bacterial viabilities of (C) *Amp<sup>r</sup> E. coli*, (D) *E. faecalis* treated with PBS,  $MoS_2$ - $\alpha$ -CD, BNN6, and  $MoS_2$ -BNN6 without or with 808 nm laser irradiation (1.0  $W/cm^2$ , 10 min). Reproduced with permission from [157], copyright 2018 WILEY-VCH Verlag GmbH & Co. KGaA, Weinheim.

Aside from the photo-induced germicidal ability, the peroxidase-like activity of MoS<sub>2</sub>/MoSe<sub>2</sub> nanosheets has also been verified. Our group constructed functionalized nano-MoS<sub>2</sub> with peroxidase catalytic and NIR PTT for synergetic antibacterial [143]. Besides, the imbalance of bacterial flora may increase resistance, which demands the development of strain-selective bactericidal strategies. To this end, Qu's groups designed an intelligent photo-responsive Gram- selective antibacterial system citraconic anhydride-modified MoS<sub>2</sub> [185]. This nanosystem possesses charge-selective antibacterial potential because the surface charge could be modulated by altering light irradiation time, and the simultaneous lower pH value would activate the peroxidase-like activity of MoS<sub>2</sub> nanozymes as well as increase antibacterial effects. In addition, Huang *et al.* used carboxyl-modified silk fibroin as the exfoliating agent to high-yield synthesize thin-layer MoSe<sub>2</sub> nanosheets, and revealed that the superior peroxidase-like activity of MoSe<sub>2</sub> nanosheets could effectively resist bacterial infections and promote wound healing [159]. Furthermore, the antibacterial activity of WX<sub>2</sub> nanosheets has also been valued in recent years [186]. Bang *et al.* designed a facile and effective exfoliation technique to fabricate WX<sub>2</sub> (X=S or Se) nanosheets by using single-stranded DNA (ssDNA) of high ssDNA molecular weight, and investigated the antibacterial activity of the as-prepared WX<sub>2</sub>. They found that WSe<sub>2</sub>-ssDNA nanosheets had remarkable antibacterial activity due to their strong GSH oxidation capacity, which suggested the ROS-independent oxidative stress antibacterial properties of WSe<sub>2</sub>-ssDNA nanosheets [65, 85].

### 3.2 Metal-Based 2D Antibacterial Nanomaterials

It has been demonstrated that metallic nanoparticles, including Ag, Au [187], Ti, Cu [188], Zn [189], Mg [190-192] and Ni [192], exhibit potential antibacterial activity. However, compared to 2D nanomaterials, these metallic nanoparticles show compromised bactericidal efficiency due to its small specific surface area and fewer surface-active sites. Therefore, the strategy to overcome the shortcomings and obtain high-performance antibacterial effect of metal alone is either to decorate 2D nanosheets with metallic nanoparticles or prepare 2D metallic nanosheets [193-195]. Towards this direction, Mo *et al.* prepared Pd@Ag nanosheets through the reduction of Ag ions with formaldehyde on the surface of Pd nanosheets. It could realize a synergetic antibacterial effect of PTT and Ag ions released under the

irradiation of NIR light (**Figure 9A**) [162]. The amounts of released Ag from Pd@Ag nanosheets were monitored by inductively coupled plasma mass spectrometry (ICP-MS), and results showed that NIR irradiation could significantly increase silver release compared to non-irradiated controls (**Figure 9B**). Interestingly, the bacteria viability indicated that NIR laser or Pd@Ag nanosheets alone did not kill bacteria effectively, while Pd@Ag nanosheets upon NIR irradiation could realize efficient bacteria-killing effect as almost 100% bacteria was killed after the synergistic treatment for 10 min (**Figure 9C, D**). Therefore, Pd@Ag nanosheets with outstanding photothermal conversion effect could not only generate heat to kill bacteria, but also destroy the bacterial membrane with released Ag ions under the irradiation of NIR light. Recently, 2D nanosized metallic oxides, such as TiO<sub>2</sub> [196], CuO [188], and ZnO [197, 198], have shown excellent antibacterial performance and drawn widespread attention due to their favorable photocatalytic activities, benign biosafety, strong oxidizing power, and rich surface-active sites. Among them, ultrathin TiO<sub>2</sub> nanosheets are confirmed as the most outstanding antibacterial, which is attributed to their numerous advantages, such as low-cost, low-toxicity, good stability, as well as robust oxidizing capability. In general, TiO<sub>2</sub> nanosheets have three phase structure: brookite, rutile and anatase. Among them, anatase TiO<sub>2</sub> nanosheets have been widely applied as a photocatalyst [196]. To explore the in-depth capacity of TiO<sub>2</sub>, Arnab *et al.* prepared MoS<sub>2</sub>-TiO<sub>2</sub> nanocomposites with significant antibacterial ability [165]. In addition, Ma *et al.* fabricated ultrathin Fe<sub>3</sub>O<sub>4</sub>-TiO<sub>2</sub> nanosheets (Fe<sub>3</sub>O<sub>4</sub>-TNS) using lamellar reverse micelles and solvothermal method for efficient antibacterial application [199]. On the one hand, Fe<sub>3</sub>O<sub>4</sub>-TNS could effectively capture photo-induced electron and accelerate the separation of electron-hole pairs. On the other hand, Fe<sub>3</sub>O<sub>4</sub>-TNS showed superior antibacterial activity to *E. coli* under the irradiation of solar light. Moreover, Wang *et al.* designed a bifunctional layered Cu<sub>2</sub>S nanoflowers/biopolymer-incorporated electrospun membrane for tumor therapy and as a source of Cu ions for wound healing [89]. Despite the tremendous antibacterial potential of metal-based nanomaterial shown from these studies, it is important to investigate their cytotoxicity and immune response effect on human cells. Therefore, metal-based antibacterial nanomaterials deserve further research regarding their *in vivo* biological effect before clinical sterilization application.

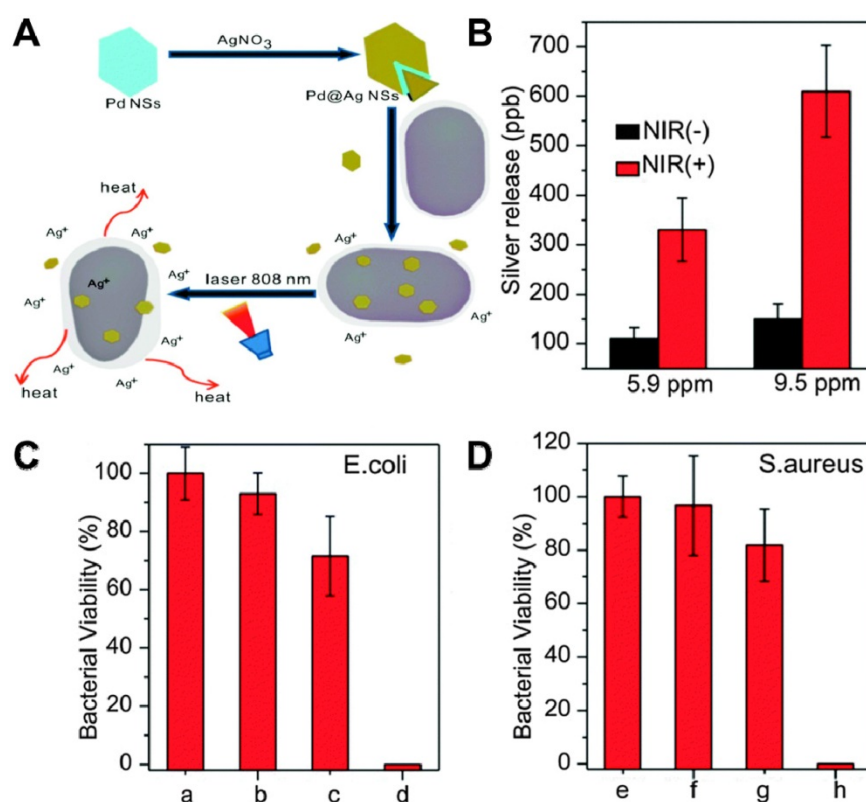


**Figure 9.** (A) Schematic illustration of the Pd@Ag nanosheets for synergistic treatment of bacteria. (B) Silver released from 5.9 and 9.5 ppm of Pd@Ag nanosheets with and without light irradiation. Histograms of (C) *E. coli* and (D) *S. aureus* viability treated with Pd@Ag nanosheets under NIR irradiation. Reproduced with permission from [162], copyright 2015 The Royal Society of Chemistry.

### 3.3 Nitride-Based Antibacterial Nanomaterials

$C_3N_4$  was first synthesized by Berzelius in the 1830s, subsequently Liebig named it “melon” [111]. Recently,  $g-C_3N_4$  nanosheets, a burgeoning nitride-based polymeric semiconductor material with laminar structure and narrow bandgap, have attracted giant attention on the antibacterial field owing to their highly efficient photocatalytic performance, large surface area, good chemical stability and adjustable electron band structure [200]. Wu *et al.* once synthesized an Ag/polydopamine/ $g-C_3N_4$  bio-photocatalyst antibacterial agent using *in situ* reduction method (Figure 10A) [170]. On the one hand, the photocatalytic activity of Ag/polydopamine/ $g-C_3N_4$  was improved through Ag NPs and polydopamine under the irradiation of visible light, followed by the generation of abundant ROS (particularly  $\bullet OH$ ). On the other hand, light could accelerate the release of Ag ions. Finally, the Ag/polydopamine/ $g-C_3N_4$  displayed excellent antibacterial activity by a synergistic effect between Ag ions and PCT of  $g-C_3N_4$  nanosheets (Figure 10B). Simultaneously, this bio-photocatalyst has commendable biocompatibility and outstanding stable antibacterial activity (Figure 10C). To further advance the use of  $g-C_3N_4$  as photocatalysts, Wang *et*

*al.* firstly designed a novel metal-free heterojunction through coating cyclooctasulfur ( $a-S_8$ ) with rGO and  $g-C_3N_4$  nanosheets for photocatalytic disinfection under visible light [113]. They found that the photocatalytic bacteria inactivation mechanism of this nano-heterojunction mainly through photogenerated ROS in an aerobic environment or through electron transfer induced oxidative stress under anaerobic conditions (Figure 10D). Intriguingly, the results showed that a  $S_8$  (core)/rGO (inner shell)/ $g-C_3N_4$  (outer shell) (CNRGOS<sub>8</sub>) arrangement exhibited higher antibacterial effect under aerobic conditions (Figure 10E), whereas a  $S_8$  (core)/ $g-C_3N_4$  (inner shell)/rGO (outer shell) (RGOCS<sub>8</sub>) arrangement showed excellent antibacterial ability under anaerobic conditions (Figure 10F). In addition, Li and co-workers fabricated  $g-C_3N_4$  nanosheets functionalized hydrophilic composite membranes, and found that the antibacterial ability largely increased with the modification of  $g-C_3N_4$  nanosheets [166]. Furthermore, Wang *et al.* reported that vanadate quantum dots-inset  $g-C_3N_4$  (vanadate QDs/ $g-C_3N_4$ ) nanosheets showed faster photocatalytic disinfection with abundant ROS compared to bare  $g-C_3N_4$  nanosheets [171]. Moreover, to reduce the toxicity risk of heavy metal species, Chen’s groups created a novel all-organic self-assembled semiconductor photocat-

alytic nanomaterial  $C_3N_4$ /PDINH heterostructure for photocatalytic antibacterial by recrystallization of PDINH (perylene-3,4,9,10-tetracarboxylic diimide) on the surface of  $C_3N_4$  nanosheets *in situ* [201]. Intriguingly, they found that the absorption spectrum of heterostructure were greatly extended from UV to NIR, enhancing the photocatalytic effect to generate more ROS for better bactericidal, while revealing low-toxicity to healthy tissue cells. Simultaneously, the  $C_3N_4$ /PDINH heterostructure could quickly cure the *in vivo* infected area, and promote wound regeneration. Taken together, although  $C_3N_4$ -based photocatalyst has reported in various biomedical fields, its photocatalytic efficiency is still relatively low to meet the requirements of practical applications. Therefore, enhancing the catalytic efficiency of  $C_3N_4$  nanosheets in the future is highly expected.

### 3.4 Black Phosphorus-Based Antibacterial Nanomaterials

BP, a rising star of 2D nanomaterials family, has attracted great attention since 2014 [202, 203]. Recently, 2D BP nanosheets have attracted widespread attention due to their fascinating thermal/optical/electrical performance, and the weak Van der Waals forces allow its easy exfoliation into ultrathin 2D nanosheets [204, 205]. Owing to their metal-free semiconductor features and thickness-dependent band gap, BP nanosheets possess a very

broad light absorption across entire visible regions [206]. Therefore, 2D layered BP nanosheets can be used to produce  $^1O_2$  under visible light, which can be applied to PDT [207]. Towards this direction, Mao *et al.* fabricated a BP-based hybrid hydrogel (CS-BP) therapeutic system for repeatable PDT disinfection and promote wound healing (**Figure 11A**) [39]. They used electron spin resonance (ESR) spectra to trap  $^1O_2$ , and found that only CS-BP hydrogel could rapidly generate  $^1O_2$  under visible light irradiation (**Figure 11B**). Meanwhile, under light irradiation with simulated sunlight, CS hydrogel showed moderate bactericidal efficacy while CS-BP could kill most bacteria (*E. coli* and *S. aureus*) within 10 min (**Figure 11C, D**). Moreover, the CS-BP hydrogel still maintain favorable reusable antibacterial efficacy even after four repeatedly challenge with high concentrations of *S. aureus* (**Figure 11E**). In addition, Huang *et al.* prepared thin-layer BP@ silk fibroin nanosheets with subtle solution-processability using silk fibroin as an exfoliating agent, and revealed that BP@ silk fibroin nanosheets not only could be fabricated into various formats but also show excellent PTT disinfection and wound repair ability [92]. Based on the above attractive findings, BP-based nanomaterials hold great promise for material science, biomedicine, and biotechnology in the future.

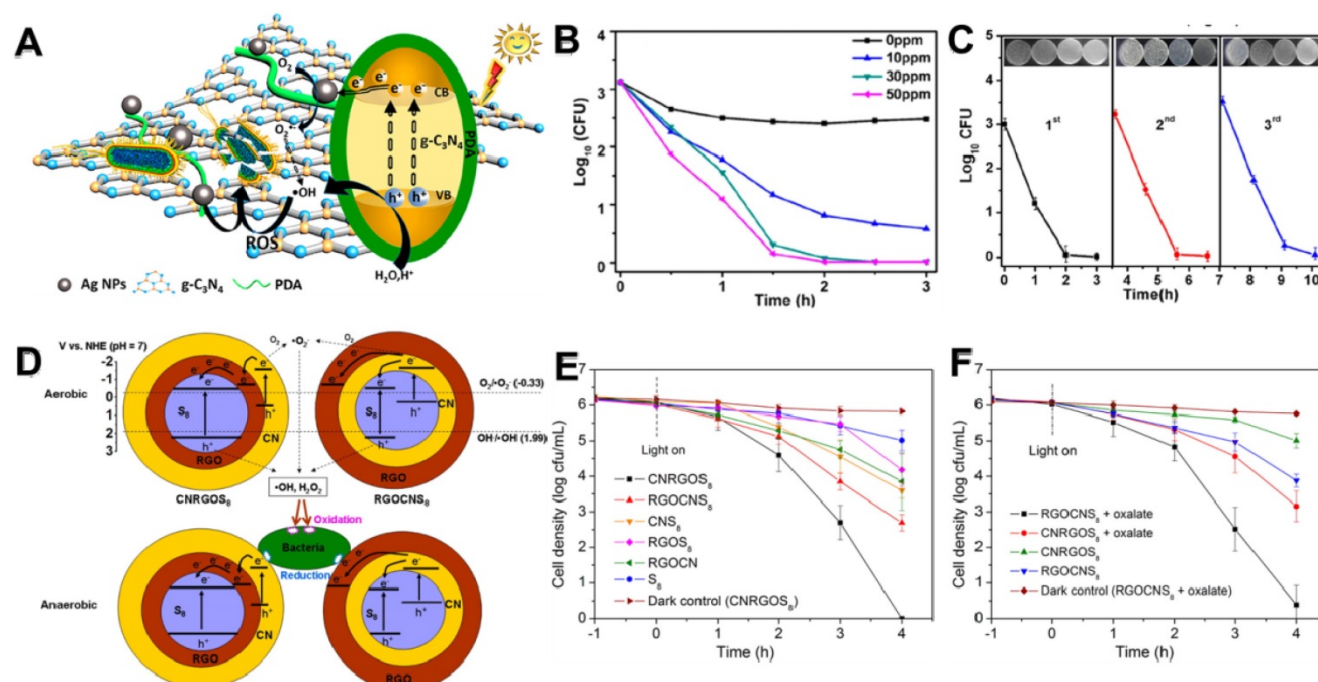


**Figure 10.** (A) Bactericidal mechanism for Ag/PDA/g- $C_3N_4$  bio-photocatalyst. (B) Bactericidal time curve profiles of *E. coli* treated with different concentrations of Ag/PDA/g- $C_3N_4$  (1:2) within 3 h. (C) Three-cycle run experiments of photocatalytic disinfection of 30 ppm Ag/PDA/g- $C_3N_4$  (1:2) under visible-light irradiation. Reproduced with permission from [170], copyright 2018 American Chemical Society. (D) Schematic illustration of the VLD photocatalytic bacterial inactivation mechanisms of CNRGOS<sub>8</sub>/RGO/CNS<sub>8</sub> in aerobic condition, and CNRGOS<sub>8</sub>/RGO/CNS<sub>8</sub> in anaerobic condition. Photocatalytic inactivation efficiency against *E. coli* K-12 without (E) and with (F) 0.5 mmol/L sodium oxalate in the presence of the samples (100 mg/L) in anaerobic condition under visible light irradiation. Reproduced with permission from [113], copyright 2018 American Chemical Society.

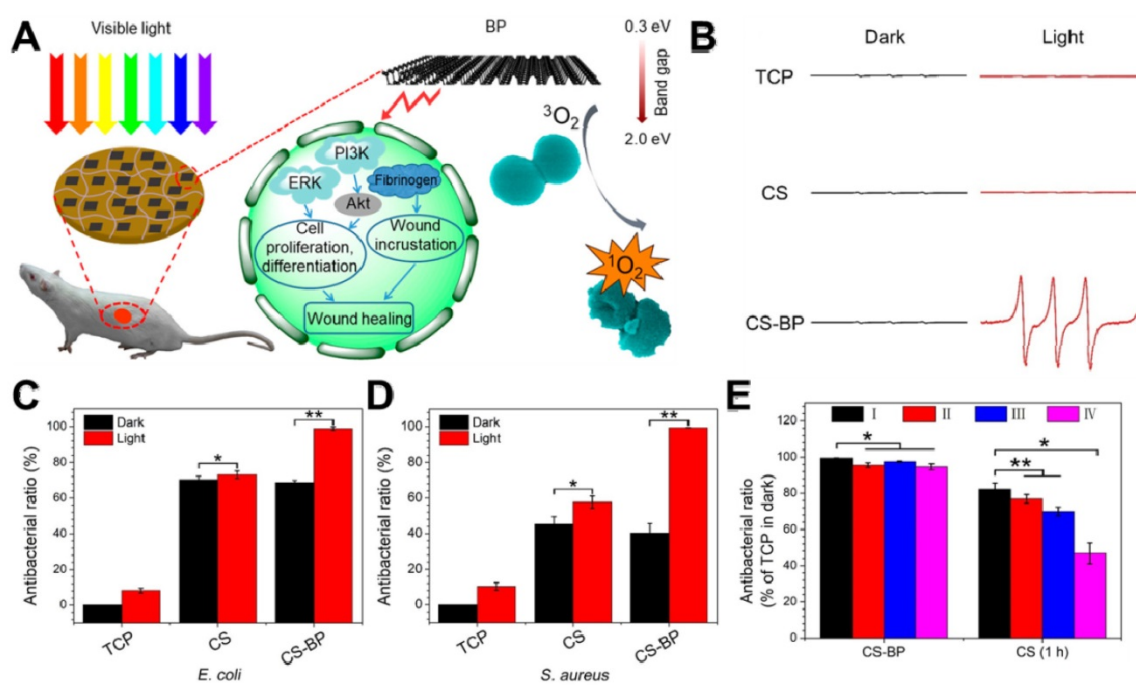


**Figure 11.** (A) Sterilization under visible light irradiation and the process of stimulating skin cell behaviors that can promote the regenerative activities of the skin cells and actively participate in skin regeneration to accelerate bacteria-accompanied wound healing using BP-based hydrogel. (B) Electron spin resonance spectra. The corresponding abilities of the samples (TCP, the CS hydrogel, and the CS-BP hydrogel) to kill *E. coli* (C) and *S. aureus* (D); (E) Corresponding abilities of the samples to kill *S. aureus*; the CS-BP hydrogel and CS hydrogel were repeatedly challenged with *S. aureus* under simulated sunlight for 10 min and in the darkness for 1 h, respectively, repeatedly up to four times. Reproduced with permission from [39], copyright 2018 American Chemical Society.

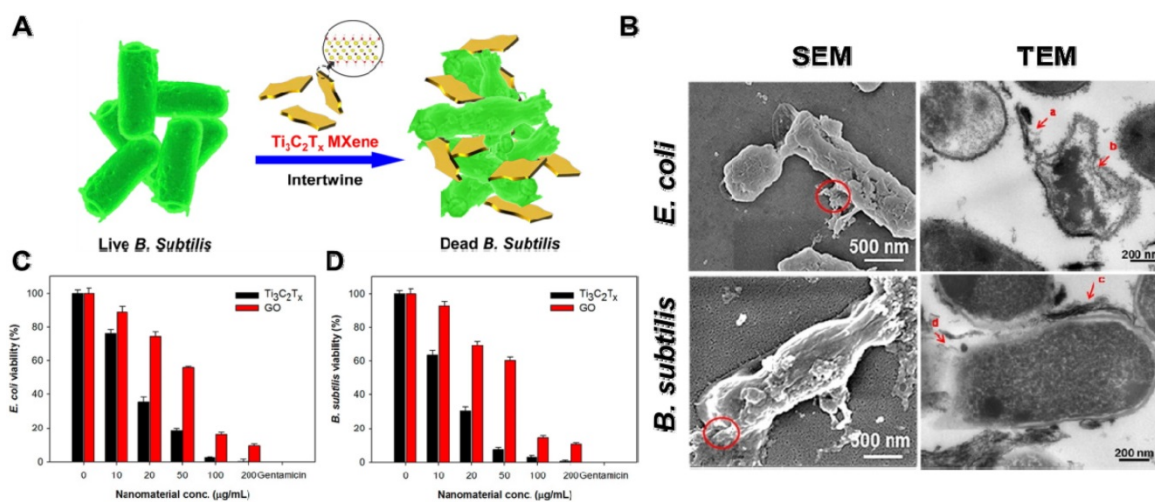


**Figure 12** (A) Schematic illustration of the interaction between  $Ti_3C_2T_x$  and bacteria. (B) SEM and TEM images of *E. coli* and *B. subtilis* cells treated with  $Ti_3C_2T_x$  MXenes. Cell viability measurements of (C) *E. coli* and (D) *B. subtilis* treated with an aqueous suspension of  $Ti_3C_2T_x$  MXenes. Reproduced with permission from [173], copyright 2016 American Chemical Society.

### 3.5 MXenes Antibacterial Nanomaterials

MXenes are a very new member of 2D transition metal carbides/nitrides with a general formula of  $M_{n+1}A_nT_x$  (M stands for transition metal, A is carbon or nitrogen, and T is surface-terminating functional groups, such as -OH, -O, or -F) [25, 208]. So far, approximate 70 kinds of MXenes have been reported, among which  $Ti_3C_2T_x$  is the most representative MXenes material [209]. Recently, studies demonstrated that  $Ti_3C_2T_x$  MXenes nanosheets

display outstanding antibacterial performances owing to their ultrathin lamellar morphology and unique physiochemical properties [209-211]. For instance, Rasool *et al.* synthesized  $Ti_3C_2T_x$  MXenes colloidal suspension using ultrasonication in argon (Ar) gas and first demonstrated their outstanding antibacterial behavior towards *E. coli* and *B. subtilis* (Figure 12A) [173, 212]. In comparison to GO, the  $Ti_3C_2T_x$  MXenes nanosheets displayed distinct dose-dependent bactericidal efficacy, and up to 98% of bacterial were killed after incubated with 200  $\mu\text{g}/\text{mL}$   $Ti_3C_2T_x$  for 4 h

(Figure 12C, D). According to the SEM and TEM images, they proposed that the antibacterial mechanism of  $Ti_3C_2T_x$  MXenes nanosheets were ascribed to the synergism of sharp edge induced membrane damage and electron transfer rendered oxidative stress (Figure 12B). Then, they further fabricated  $Ti_3C_2T_x$  MXenes nanosheets coated with polyvinylidene fluoride (PVDF) membranes by vacuum-assisted filtration method and further studied their antibacterial ability towards *E. coli* and *B. subtilis* [174]. Compared to fresh  $Ti_3C_2T_x$ /PVDF membranes, the aged  $Ti_3C_2T_x$ /PVDF membranes were more active in enhancing the overall antibacterial properties owing to the synergistic effect between  $Ti_3C_2T_x$  nanosheets and the formation of anatase  $TiO_2$  nanocrystals with sharp edges. Moreover, Shamsabadi *et al.* reported that colloidal  $Ti_3C_2T_x$  MXenes nanosheets showed both size- and exposure time-dependent antibacterial properties. They found that the direct interactions between sharp edges of  $Ti_3C_2T_x$  MXenes nanosheets and bacteria membrane cause serious damage to the bacterial membrane [212]. Taking into consideration that MXenes' chemical behavior depends on the kind of transition metals (such as Mo, Nb, V) and surface-terminating functional groups, different physicochemical properties are closely relevant to antibacterial effects. Therefore, fine regulated ultrathin MXenes nanosheets will open a wide door for multiple and extensive application in antibacterial coatings and biomedical applications.

### 3.6 Others 2D NBG Antibacterial Nanomaterials

In addition to the above-mentioned 2D NBG antibacterial nanomaterials, some other new members of 2D nanomaterials, such as layered double hydroxides (LDHs) [213–216], laponite (Lap) [217, 218], hexagonal boron nitride (BN) [176], III<sub>2</sub>-VI<sub>3</sub> compounds ( $In_2Se_3$ ,  $Bi_2Se_3$ ,  $Sb_2Se_3$ ) [90, 177, 219, 220], and  $RuO_2$  have also been deemed as promising antibacterial agents. For example, Wang *et al.* prepared various morphology of lysozyme modified LDHs through tuning the ratio of cations, and found that bloom flower structure of LDHs not only could load more lysozyme but also adhere to more bacteria, which show excellent antibacterial activity and wound healing ability [175]. Moreover, Ghadiri *et al.* fabricated a Laponite/mafenide/alginate (Lap/Maf/Alg) film with remarkable antibacterial effects and good wound healing applications [221]. Furthermore, Zhu *et al.* synthesized large quantities of  $In_2Se_3$  nanosheets using a solvent exfoliation method. Their results revealed that the  $In_2Se_3$  nanosheets possess excellent photothermal performance, which causes

significant antibacterial effect [177]. Similarly, Miao *et al.* synthesized new atomically thin antimony  $Sb_2Se_3$  nanosheets using a liquid exfoliation method, which could kill bacteria through physical contact destruction and short-time hyperthermia sterilization under laser irradiation [90]. Therefore, various 2D antibacterial materials with excellent bacteria inhibition efficacy should gain more researchers' attention.

## 4. Conclusions and Future Perspectives

In recent years, the increasing of bacteria multidrug resistance to traditional antibiotics has greatly hampered the development of antibacterial applications. Fortunately, various emerging 2D NBG, which show promising potential and good opportunities in addressing antibacterial issues, have demonstrated their excellent ability to kill drug-resistant bacteria. In this review, we systematically summarize the research progress of versatile 2D NBG from their antibacterial mechanisms to materials classification, and the effect of unique physicochemical properties on their antibacterial applications. Similar to graphene, 2D NBG also has features such as high specific surface area, better stability, and good biosafety, which make them one of the most advanced, attractive, and promising antibacterial nano-agents. Currently, the existing antibacterial mechanisms of 2D NBG mainly include physical contact destruction, oxidative stress, photo-induced (photothermal, photocatalytic and photodynamic) heat/ROS production to damage cellular components, controlled drugs or metallic ions releasing, and multi-mode synergistic antibacterial. Among them, synergistic antibacterial is the most effective bactericidal method, and photo-induced antibacterial, especially photocatalytic antibacterial, has attracted far-ranging attention in recent years. Furthermore, we also discuss the effect of the physicochemical characteristic of 2D NBG on antibacterial effects. In addition, we have divided the 2D NBG into the following categories: TMDC/Os, Metal-based, Nitride-based, BP, MXenes and other 2D NBG antibacterial nanoagents. Although extensive research demonstrated that 2D NBG has excellent antibacterial activities, studies regarding the clinical translation of the 2D NBG are still rare. Therefore, in order to realize more practical application, it requires us to focus on several important issues in the future:

I) *The systematical evaluation of the biosafety of 2D NBG is all-important before being translated into clinical practice.* Currently, 2D NBG has been exhibited tremendous potential in antibacterial, water disinfection, wound healing, and other biomedical filed. However, biosafety consideration is a

prerequisite for the clinical antibacterial translation of these 2D nanomaterials. Although some reports have been conducted to investigate the dosage, incubation time, and surface modification-related biosafety of 2D NBG, such research is still insufficient and remains controversial for the biosafety evaluation of 2D NBG [222]. Most recent studies have demonstrated that 2D NBG presents good biocompatibility and low toxic effects after suitable functionalization, however, their long-term biological effects *in vivo* still unexplored [223, 224]. Firstly, although metal or metallic ions possess apparent antibacterial properties, studies of exploring and reducing their *in vivo* long-term toxicity are needed. Secondly, to accelerate the metabolism of 2D NBG, we can improve their biodegradability through surface functionalization or design ultrasmall size of 2D NBG to make them more easily cleared out of the body [225]. Thirdly, developing 2D NBG with targeting antibacterial ability could not only specifically target bacteria to improve antibacterial efficiency but also reduce their toxicity and side effects to normal tissues. Finally, the mechanism for clearance pathways and other biological effects of 2D nanomaterials are still not clear. Thus, putting all these unresolved biosafety issues in the first place for deep investigation is essential, which is beneficial for their future preclinical or clinical antibacterial application.

II) *The deeper exploration of the interactions between 2D NBG-bacteria interfaces and related antibacterial mechanisms.* To date, lots of antibacterial mechanisms of 2D NBG have been widely recognized, but most of the mechanism studies are far from comprehensive. Thus, it is essential to deeply understand the antibacterial mechanisms and explore the interactions between nanomaterials and intracellular components of microorganisms.

III) *The optimization of the physicochemical properties of 2D NBG nanomaterials for enhancing antibacterial effects.* As mentioned above, size, shape, phase structure, number of layers and surface functional modification, all of them affect antibacterial activities. For example, different size of MoS<sub>2</sub> nanosheets possesses different drugs load capacity, leading to different antibacterial activities. Moreover, the shape-dependent antibacterial effects of VS<sub>2</sub> nanosheets were also revealed. Therefore, the systematic study on unique physicochemical properties relevant to the antibacterial effect should be carried out to gain the satisfying antibacterial efficiency of 2D NBG for better preclinical use.

IV) *The exploration of the optimal modality of synergistic antibacterial.* In this review, we have summarized various combined modalities for synergistic bactericidal. However, no reliable research

has compared these synergistic therapeutic strategies together, causing some studies to randomly combine several treatment strategies to improve antibacterial efficacy. In addition, most of the current *in vivo* researches mainly focus on superficial wound healing, the infection in the deep site of tissue is still rarely studied. Furthermore, the ways of drug delivery also play an important role in improving the synergistic antibacterial effects. Therefore, to obtain the optimal synergistic modality of synergistic antibacterial, it is needed to compare existing synergistic antibacterial effect under the same experimental conditions or propose new synergy mechanisms of 2D NBG.

V) *The promotion of the clinical translation of 2D NBG fungicide.* Currently, various 2D NBG antibacterial nanoagents were studied by researchers, but too few clinic antibacterial agents were developed. Therefore, their clinic translation process still remains to be a giant challenge. Therefore, tremendous efforts are needed to facilitate the clinical translation of 2D NBG.

VI) *The optimization of antibacterial effects of 2D NBG by computational simulation.* Currently, with the explosive development of science and technology, computers can do exactly what humans cannot do through simulations. For example, Fan's group using coarse-grained molecular dynamics simulations studied the physical and mechanical interaction between lipid liposomes and hydrophobic nanosheets [226]. They found that the size and the orientation of 2D nanomaterials affect the interaction between cells and nanomaterials, which is a good supplement of the experiment. Based on it, we can further study the unresolved antibacterial mechanisms by the combination of computational simulation and theoretical calculation.

Taken together, we believe that this review regarding 2D NBG antibacterials can not only deepen researchers' interest in the antibacterial field, but also provide a new insight in exploring the unknown bactericidal mechanism. We hope that more research can be carried out to develop new types of safe 2D NBG antibacterials for future clinical transformation.

## Abbreviations

2D NBG: two-dimensional nanomaterials beyond graphene; ATP: adenosine triphosphate; Ar: argon; *B. subtilis*: *Bacillus subtilis*; BP: black phosphorus; B: boron; BNN6: N,N'-di-sec-butyl-N,N'-dinitroso-1,4-phenylenediamine; CFU: colony-forming unit; CB: conduction band; Cys: cysteine; CS: chitosan; CNRGOS<sub>8</sub>: S<sub>8</sub>(core)/rGO(inner shell)/g-C<sub>3</sub>N<sub>4</sub>(outer shell); DNA: deoxyribonucleic acid; DCFDA: 2',7'-dichlorofluorescein diacetate; *E. coli*: *Escherichia coli*; e: electrons; FLV-MoS<sub>2</sub>: few-layered

vertically aligned MoS<sub>2</sub>; Fe<sub>3</sub>O<sub>4</sub>-TNS: Fe<sub>3</sub>O<sub>4</sub>-TiO<sub>2</sub> nanosheets; GSH: glutathione; GSSG: glutathione disulfide; Gram<sup>-</sup>: Gram-negative; Gram<sup>+</sup>: Gram-positive; GNR@LDH: gold nanorod@layered double hydroxide; g-C<sub>3</sub>N<sub>4</sub>: graphitic carbon nitride; H<sub>2</sub>O<sub>2</sub>: hydrogen peroxide; h<sup>+</sup>: holes; h-BN: hexagonal boron nitride; ICP-MS: inductively coupled plasma mass spectrometry; LDHs: layered double hydroxides; LAP: laponite; lyso: lysozyme; MRSA: methicillin-resistant *S. aureus*; MXenes: transition metal carbides; NIR: near-infrared; NSs: nanosheets; •OH: hydroxyl radicals; •O<sub>2</sub><sup>-</sup>: superoxide anions; <sup>1</sup>O<sub>2</sub>: singlet molecular oxygen; PTT: photothermal therapy; PCT: photocatalytic therapy; PDT: photodynamic therapy; PDDA: poly diallyldimethylammonium; PPMS: poly (4-pyridonemethylstyrene); *P. aeruginosa*: *Pseudomonas aeruginosa*; PDA: polydopamine; Pen: penicillin; PEG: polyethylene glycol; PPMS: poly (4-pyridonemethylstyrene); PDDA: polyelectrolyte poly(diallyldimethylammonium chloride); PDMS: polydimethylsiloxane; PDINH: (perylene-3,4,9,10-tetracarboxylic diimide); PVDF: polyvinylidene fluoride; QDs: quantum dots; RNA: ribonucleic acid; ROS: reactive oxygen species; rGO-WS<sub>2</sub>: reduced graphene oxide-tungsten disulphide; RGOCNSs: S<sub>8</sub>(core)/g-C<sub>3</sub>N<sub>4</sub>(inner shell)/rGO(outer shell); SEM: scanning electron microscope; ssDNA: single-stranded DNA; a-S<sub>8</sub>: cyclooctasulfur; TEM: transmission electron microscope; TEG: tetraethylene glycol; TMDCs: transition metal dichalcogenides; TMDOs: transition metal oxides; TEG: tetraethylene glycol; UV: ultra violet; VB: valence band.

## Acknowledgments

This work was supported by the National Basic Research Program of China (2016YFA02021600 and 2018YFA0208900), the National Natural Science Foundation of China (51822207, 51772292, 31571015, 11621505, and 51772293), Chinese Academy of Sciences Youth Innovation Promotion Association (2013007), and CAS Key Research Program of Frontier Sciences (QYZDJ-SSW-SLH022).

## Competing Interests

The authors have declared that no competing interest exists.

## References

- Medzhitov R. Recognition of microorganisms and activation of the immune response. *Nature*. 2007; 449: 819-26.
- Parvez MK, Parveen S. Evolution and Emergence of Pathogenic Viruses: Past, Present, and Future. *Intervirology*. 2017; 60: 1-7.
- Martens EC, Neumann M, Desai MS. Interactions of commensal and pathogenic microorganisms with the intestinal mucosal barrier. *Nat Rev Microbiol*. 2018; 16: 457-70.
- Ling LL, Schneider T, Peoples AJ, Spoering AL, Engels I, Conlon BP, et al. A new antibiotic kills pathogens without detectable resistance. *Nature*. 2015; 517: 455-9.
- Kohanski MA, Dwyer DJ, Hayete B, Lawrence CA, Collins JJ. A common mechanism of cellular death induced by bactericidal antibiotics. *Cell*. 2007; 130: 797-810.
- Ter Kuile BH, Hoeksema M. Antibiotic Killing through Incomplete DNA Repair. *Trends Microbiol*. 2018; 26: 2-4.
- Kohanski MA, Dwyer DJ, Collins JJ. How antibiotics kill bacteria: from targets to networks. *Nat Rev Microbiol*. 2010; 8: 423-35.
- Anand A, Unnikrishnan B, Wei S, Chou C, Zhang L, Huang C. Graphene oxide and carbon dots as broad-spectrum antimicrobial agents—a minireview. *Nanoscale Horiz*. 2019; 4: 117-37.
- He X, Xiong LH, Zhao Z, Wang Z, Luo L, Lam JWY, et al. AIE-based theranostic systems for detection and killing of pathogens. *Theranostics*. 2019; 9: 3223-48.
- Pope CF, Sullivan DM, McHugh TD, Gillespie SH. A practical guide to measuring mutation rates in antibiotic resistance. *Antimicrob Agents Chemother*. 2008; 52: 1209-14.
- Andersson DI. Improving predictions of the risk of resistance development against new and old antibiotics. *Clin Microbiol Infect*. 2015; 21: 894-8.
- Ragheb MN, Thomason MK, Hsu C, Nugent P, Gage J, Samadpour AN, et al. Inhibiting the Evolution of Antibiotic Resistance. *Mol Cell*. 2019; 73: 157-65.
- Syal K, Mo M, Yu H, Iriya R, Jing W, Guodong S, et al. Current and emerging techniques for antibiotic susceptibility tests. *Theranostics*. 2017; 7: 1795-805.
- Chen Z, Wang Z, Ren J, Qu X. Enzyme mimicry for combating bacteria and biofilms. *Acc Chem Res*. 2018; 51: 789-99.
- Qiao Z, Yao Y, Song S, Yin M, Luo J. Silver nanoparticles with pH induced surface charge switchable properties for antibacterial and antibiofilm applications. *J Mater Chem B*. 2019; 7: 830-40.
- Dai X, Zhao Y, Yu Y, Chen X, Wei X, Zhang X, et al. All-in-one NIR-activated nanoplatforms for enhanced bacterial biofilm eradication. *Nanoscale*. 2018; 10: 18520-30.
- Mendoza RA, Hsieh J-C, Galiano RD. The Impact of Biofilm Formation on Wound Healing. *Wound Healing-Current Perspectives*. IntechOpen; 2019: 235-250.
- Albada B, Metzler-Nolte N. Highly potent antibacterial organometallic peptide conjugates. *Acc Chem Res*. 2017; 50: 2510-8.
- Wang C, Wang M, Xu T, Zhang X, Lin C, Gao W, et al. Engineering Bioactive Self-Healing Antibacterial Exosomes Hydrogel for Promoting Chronic Diabetic Wound Healing and Complete Skin Regeneration. *Theranostics*. 2019; 9: 65-76.
- Dizaj SM, Lotfipour F, Barzegar-Jalali M, Zarrintan MH, Adibkia K. Antimicrobial activity of the metals and metal oxide nanoparticles. *Mater Sci Eng C*. 2014; 44: 278-84.
- Cattoir V, Felden B. Future Antibacterial Strategies: From Basic Concepts to Clinical Challenges. *J Infect Dis*. 2019; 220: 350-60.
- Miller KP, Wang L, Benicewicz BC, Decho AW. Inorganic nanoparticles engineered to attack bacteria. *Chem Soc Rev*. 2015; 44: 7787-807.
- Chen H, Gu Z, An H, Chen C, Chen J, Cui R, et al. Precise nanomedicine for intelligent therapy of cancer. *Sci China: Chem*. 2018; 61: 1503-52.
- Jiang X, Wang C, Fitch S, Yang F. Targeting Tumor Hypoxia Using Nanoparticle-engineered CXCR4-overexpressing Adipose-derived Stem Cells. *Theranostics*. 2018; 8: 1350-60.
- Liu Z, Lin H, Zhao M, Dai C, Zhang S, Peng W, et al. 2D Superparamagnetic Tantalum Carbide Composite MXenes for Efficient Breast-Cancer Theranostics. *Theranostics*. 2018; 8: 1648-64.
- Li Y, Liu X, Tan L, Cui Z, Jing D, Yang X, et al. Eradicating Multidrug-Resistant Bacteria Rapidly Using a Multi-Functional g-C<sub>3</sub>N<sub>4</sub>@Bi<sub>2</sub>S<sub>3</sub> Nanorod Heterojunction with or without Antibiotics. *Adv Funct Mater*. 2019; 29: 1900946.
- Wang Y, Jin Y, Chen W, Wang J, Chen H, Sun L, et al. Construction of nanomaterials with targeting phototherapy properties to inhibit resistant bacteria and biofilm infections. *Chem Eng J*. 2019; 358: 74-90.
- Chitgupi U, Qin Y, Lovell JF. Targeted Nanomaterials for Phototherapy. *Nanotheranostics*. 2017; 1: 38-58.
- Wang LS, Gupta A, Rotello VM. Nanomaterials for the treatment of bacterial biofilms. *ACS Infect Dis*. 2016; 2: 3-4.
- Beyth N, Hourri-Haddad Y, Domb A, Khan W, Hazan R. Alternative Antimicrobial Approach: Nano-Antimicrobial Materials. *Evid-Based Complement & Alternat Med*. 2015; 2015: 1-16.
- Hemeg HA. Nanomaterials for alternative antibacterial therapy. *Int J Nanomedicine*. 2017; 12: 8211-25.
- Gu Z, Zhu S, Yan L, Zhao F, Zhao Y. Graphene-based smart platforms for combined cancer therapy. *Adv Mater*. 2019; 31: 1800662.
- Li X, Robinson SM, Gupta A, Saha K, Jiang Z, Moyano DF, et al. Functional gold nanoparticles as potent antimicrobial agents against multi-drug-resistant bacteria. *ACS Nano*. 2014; 8: 10682-6.
- Sun Z, Li Y, Guan X, Chen L, Jing X, Xie Z. Rational design and synthesis of covalent organic polymers with hollow structure and excellent antibacterial efficacy. *RSC Adv*. 2014; 4: 40269-72.
- Mangadlao JD, Santos CM, Felipe MJL, de Leon ACC, Rodrigues DF, Advincula RC. On the antibacterial mechanism of graphene oxide (GO) Langmuir-Blodgett films. *Chem Commun*. 2015; 51: 2886-9.
- Liu Y, Zhao Y, Sun B, Chen C. Understanding the toxicity of carbon nanotubes. *Acc Chem Res*. 2013; 46: 702-13.
- Xu J, Yao K, Xu Z. Nanomaterials with a photothermal effect for antibacterial activities: an overview. *Nanoscale*. 2019; 11: 8680-91.

38. Wang W, Li G, Xia D, An T, Zhao H, Wong PK. Photocatalytic nanomaterials for solar-driven bacterial inactivation: recent progress and challenges. *Environ Sci Nano*. 2017; 4: 782-99.
39. Mao C, Xiang Y, Liu X, Cui Z, Yang X, Li Z, et al. Repeatable photodynamic therapy with triggered signaling pathways of fibroblast cell proliferation and differentiation to promote bacteria-accompanied wound healing. *ACS Nano*. 2018; 12: 1747-59.
40. Yang X, Yang J, Wang L, Ran B, Jia Y, Zhang L, et al. Pharmaceutical intermediate-modified gold nanoparticles: against multidrug-resistant bacteria and wound-healing application *via* an electrospun scaffold. *ACS Nano*. 2017; 11: 5737-45.
41. Zhang W, Mou Z, Wang Y, Chen Y, Yang E, Guo F, et al. Molybdenum disulfide nanosheets loaded with chitosan and silver nanoparticles effective antifungal activities: *in vitro* and *in vivo*. *Mater Sci Eng, C*. 2019; 97: 486-97.
42. Xin Q, Shah H, Nawaz A, Xie W, Akram MZ, Batool A, et al. Antibacterial carbon-based nanomaterials. *Adv Mater*. 2018; 0: 1804838.
43. Yin F, Hu K, Chen Y, Yu M, Wang D, Wang Q, et al. SiRNA Delivery with PEGylated Graphene Oxide Nanosheets for Combined Photothermal and Gene Therapy for Pancreatic Cancer. *Theranostics*. 2017; 7: 1133-48.
44. Han H, Qiu Y, Shi Y, Wen W, He X, Dong L, et al. Glypican-3-targeted precision diagnosis of hepatocellular carcinoma on clinical sections with a supramolecular 2D imaging probe. *Theranostics*. 2018; 8: 3268-74.
45. Lokese WJ, Bolkestein M, Ten Hagen TL, de Jong M, Eggermont AM, Grull H, et al. Investigation of Particle Accumulation, Chemosensitivity and Thermosensitivity for Effective Solid Tumor Therapy Using Thermosensitive Liposomes and Hyperthermia. *Theranostics*. 2016; 6: 1717-31.
46. Jacobson O, Weiss ID, Szajek LP, Niu G, Ma Y, Kiesewetter DO, et al. PET imaging of CXCR4 using copper-64 labeled peptide antagonist. *Theranostics*. 2011; 1: 251-62.
47. Ji H, Sun H, Qu X. Antibacterial applications of graphene-based nanomaterials-Recent achievements and challenges. *Adv Drug Delivery Rev*. 2016; 105: 176-89.
48. Jia Q, Yang F, Huang W, Zhang Y, Bao B, Li K, et al. Low Levels of Sox2 are required for Melanoma Tumor-Repopulating Cell Dormancy. *Theranostics*. 2019; 9: 424-35.
49. You R, Cao YS, Huang PY, Chen L, Yang Q, Liu YP, et al. The Changing Therapeutic Role of Chemo-radiotherapy for Loco-regionally Advanced Nasopharyngeal Carcinoma from Two/Three-Dimensional Radiotherapy to Intensity-Modulated Radiotherapy: A Network Meta-Analysis. *Theranostics*. 2017; 7: 4825-35.
50. Karahan HE, Wiraja C, Xu C, Wei J, Wang Y, Wang L, et al. Graphene materials in antimicrobial nanomedicine: current status and future perspectives. *Adv Healthc Mater*. 2018; 7: 1701406.
51. Bhirde AA, Liu G, Jin A, Iglesias-Bartolome R, Sousa AA, Leapman RD, et al. Combining portable Raman probes with nanotubes for theranostic applications. *Theranostics*. 2011; 1: 310-21.
52. Kurapati R, Kostarelou K, Prato M, Bianco A. Biomedical uses for 2D materials beyond graphene: current advances and challenges ahead. *Adv Mater*. 2016; 28: 6052-74.
53. Epah J, Palfi K, Dienst FL, Malacarne PF, Bremer R, Salamon M, et al. 3D Imaging and Quantitative Analysis of Vascular Networks: A Comparison of Ultramicroscopy and Micro-Computed Tomography. *Theranostics*. 2018; 8: 2117-33.
54. Sun W, Wu FG. Two-dimensional materials for antimicrobial applications: graphene materials and beyond. *Chem Asian J*. 2018; 13: 3378-410.
55. Han W, Wu Z, Li Y, Wang Y. Graphene family nanomaterials (GFNs)-promising materials for antimicrobial coating and film: A review. *Chem Eng J*. 2019; 358: 1022-37.
56. Miao H, Teng Z, Wang C, Chong H, Wang G. Recent progress in two-dimensional antimicrobial nanomaterials. *Chem Asian J*. 2019; 25: 929-44.
57. Zou X, Zhang L, Wang Z, Luo Y. Mechanisms of the antimicrobial activities of graphene materials. *J Am Chem Soc*. 2016; 138: 2064-77.
58. Alimohammadi F, Gh MS, Attanayake NH, Thenuwara AC, Gogotsi Y, Anasori B, et al. Antimicrobial properties of 2D MnO<sub>2</sub> and MoS<sub>2</sub> nanomaterials vertically aligned on graphene materials and Ti<sub>3</sub>C<sub>2</sub> MXene. *Langmuir*. 2018; 34: 7192-200.
59. Schwegheimer C, Kuehn MJ. Outer-membrane vesicles from Gram-negative bacteria: biogenesis and functions. *Nat Rev Microbiol*. 2015; 13: 605-19.
60. Brown L, Wolf JM, Prados-Rosales R, Casadevall A. Through the wall: extracellular vesicles in Gram-positive bacteria, mycobacteria and fungi. *Nat Rev Microbiol*. 2015; 13: 620-30.
61. Lu X, Feng X, Werber JR, Chu C, Zucker I, Kim J-H, et al. Enhanced antibacterial activity through the controlled alignment of graphene oxide nanosheets. *Proc Natl Acad Sci U S A*. 2017; 114: E9793-E801.
62. Hu W, Peng C, Luo W, Lv M, Li X, Li D, et al. Graphene-based antibacterial paper. *ACS Nano*. 2010; 4: 4317-23.
63. Krishnamoorthy K, Veerapandian M, Yun K, Kim SJ. New function of molybdenum trioxide nanoplates: Toxicity towards pathogenic bacteria through membrane stress. *Colloids Surf, B*. 2013; 112: 521-4.
64. Desai N, Mali S, Kondalkar V, Mane R, Hong C, Bhosale P. Chemically grown MoO<sub>3</sub> nanorods for antibacterial activity study. *J Nanomed Nanotechnol*. 2015; 6: 1000338.
65. Liu X, Duan G, Li W, Zhou Z, Zhou R. Membrane destruction-mediated antibacterial activity of tungsten disulfide (WS<sub>2</sub>). *RSC Adv*. 2017; 7: 37873-81.
66. Ouyang J, Wen M, Chen W, Tan Y, Liu Z, Xu Q, et al. Multifunctional two dimensional Bi<sub>2</sub>Se<sub>3</sub> nanodisks for combined antibacterial and anti-inflammatory therapy for bacterial infections. *Chem Commun*. 2019; 55: 4877-80.
67. Dallavalle M, Calvaresi M, Bottoni A, Melle Franco M, Zerbetto F. Graphene can wreak havoc with cell membranes. *ACS Appl Mater Interfaces*. 2015; 7: 4406-14.
68. Tu Y, Lv M, Xiu P, Huynh T, Zhang M, Castelli M, et al. Destructive extraction of phospholipids from *Escherichia coli* membranes by graphene nanosheets. *Nat Nanotechnol*. 2013; 8: 594-601.
69. Li Y, Yuan H, von dem Bussche A, Creighton M, Hurt RH, Kane AB, et al. Graphene microsheets enter cells through spontaneous membrane penetration at edge asperities and corner sites. *Proceedings of the National Academy of Sciences*. 2013; 110: 12295.
70. Chen P, Yan L-T. Physical principles of graphene cellular interactions: computational and theoretical accounts. *J Mater Chem B*. 2017; 5: 4290-306.
71. Zheng H, Ma R, Gao M, Tian X, Li Y, Zeng L, et al. Antibacterial applications of graphene oxides: structure-activity relationships, molecular initiating events and biosafety. *Sci Bull*. 2018; 63: 133-42.
72. Li YF, Ouyang SH, Tu LF, Wang X, Yuan WL, Wang GE, et al. Caffeine Protects Skin from Oxidative Stress-Induced Senescence through the Activation of Autophagy. *Theranostics*. 2018; 8: 5713-30.
73. Ji DK, Zhang Y, Zang Y, Li J, Chen GR, He XP, et al. Targeted intracellular production of reactive oxygen species by a 2D molybdenum disulfide glycosheet. *Adv Mater*. 2016; 28: 9356-63.
74. Karunakaran S, Pandit S, Basu B, De M. Simultaneous exfoliation and functionalization of 2H-MoS<sub>2</sub> by thiolated surfactants: applications in enhanced antibacterial activity. *J Am Chem Soc*. 2018; 140: 12634-44.
75. Fan J, Li Y, Nguyen HN, Yao Y, Rodrigues DF. Toxicity of exfoliated-MoS<sub>2</sub> and annealed exfoliated-MoS<sub>2</sub> towards planktonic cells, biofilms, and mammalian cells in the presence of electron donor. *Environ Sci Nano*. 2015; 2: 370-9.
76. Kim TI, Kim J, Park IJ, Cho KO, Choi SY. Chemically exfoliated 1T-phase transition metal dichalcogenide nanosheets for transparent antibacterial applications. *2D Mater*. 2019; 6: 025025.
77. Xiong Z, Zhang X, Zhang S, Lei L, Ma W, Li D, et al. Bacterial toxicity of exfoliated black phosphorus nanosheets. *Ecotoxicol Environ Saf*. 2018; 161: 507-14.
78. Bang GS, Cho S, Son N, Shim GW, Cho BK, Choi SY. DNA-assisted exfoliation of tungsten dichalcogenides and their antibacterial effect. *ACS Appl Mater Interfaces*. 2016; 8: 1943-50.
79. Yuan Z, Tao B, He Y, Liu J, Lin C, Shen X, et al. Biocompatible MoS<sub>2</sub>/PDA-RGD coating on titanium implant with antibacterial property *via* intrinsic ROS-independent oxidative stress and NIR irradiation. *Biomaterials*. 2019; 217: 119290.
80. Perreault F, de Faria AF, Nejadi S, Elimelech M. Antimicrobial properties of graphene oxide nanosheets: why size matters. *ACS Nano*. 2015; 9: 7226-36.
81. Lyon DY, Brunet L, Hinkal GW, Wiesner MR, Alvarez PJJ. Antibacterial activity of fullerene water suspensions (nC<sub>60</sub>) is not due to ROS-mediated damage. *Nano Lett*. 2008; 8: 1539-43.
82. Yang X, Li J, Liang T, Ma C, Zhang Y, Chen H, et al. Antibacterial activity of two-dimensional MoS<sub>2</sub> sheets. *Nanoscale*. 2014; 6: 10126-33.
83. Pandit S, Karunakaran S, Boda SK, Basu B, De M. High antibacterial activity of functionalized chemically exfoliated MoS<sub>2</sub>. *ACS Appl Mater Interfaces*. 2016; 8: 31567-73.
84. Kim TI, Kwon B, Yoon J, Park IJ, Bang GS, Park Y, et al. Antibacterial activities of graphene oxide-molybdenum disulfide nanocomposite films. *ACS Appl Mater Interfaces*. 2017; 9: 7908-17.
85. Navale GR, Rout CS, Gohil KN, Dharm MS, Late DJ, Shinde SS. Oxidative and membrane stress-mediated antibacterial activity of WS<sub>2</sub> and rGO-WS<sub>2</sub> nanosheets. *RSC Adv*. 2015; 5: 74726-33.
86. Tavares A, Carvalho CMB, Faustino MA, Neves MGPM, Tomé JPC, Tomé AC, et al. Antimicrobial photodynamic therapy: study of bacterial recovery viability and potential development of resistance after treatment. *Marine Drugs*. 2010; 8: 91-105.
87. Wegener M, Hansen MJ, Driessen AJM, Szymanski W, Feringa BL. Photocontrol of antibacterial activity: shifting from UV to red light activation. *J Am Chem Soc*. 2017; 139: 17979-86.
88. Chou SS, Kaehr B, Kim J, Foley BM, De M, Hopkins PE, et al. Chemically exfoliated MoS<sub>2</sub> as near-infrared photothermal agents. *Angew Chem Int Ed*. 2013; 52: 4160-4.
89. Wang X, Lv F, Li T, Han Y, Yi Z, Liu M, et al. Electrospun micropatterned nanocomposites incorporated with Cu<sub>2</sub>S nanoflowers for skin tumor therapy and wound healing. *ACS Nano*. 2017; 11: 11337-49.
90. Miao Z, Fan L, Xie X, Ma Y, Xue J, He T, et al. Liquid exfoliation of atomically thin antimony selenide as an efficient two-dimensional antibacterial nanoagent. *ACS Appl Mater Interfaces*. 2019; 11: 26664-73.
91. Ma K, Li Y, Wang Z, Chen Y, Zhang X, Chen C, et al. A core-shell gold nanorod/layered double hydroxide nanomaterial with high efficient photothermal conversion and its application in antibacterial and tumor therapy. *ACS Appl Mater Interfaces*. 2019; 11: 29630-40.
92. Huang X, Wei J, Zhang M, Zhang X, Yin X, Lu C, et al. Water-based black phosphorus hybrid nanosheets as a moldable platform for wound healing applications. *ACS Appl Mater Interfaces*. 2018; 10: 35495-502.

93. Yin W, Yan L, Yu J, Tian G, Zhou L, Zheng X, et al. High-throughput synthesis of single-layer MoS<sub>2</sub> nanosheets as a near-infrared photothermal-triggered drug delivery for effective cancer therapy. *ACS Nano*. 2014; 8: 6922-33.
94. Yu J, Yin W, Zheng X, Tian G, Zhang X, Bao T, et al. Smart MoS<sub>2</sub>/Fe<sub>3</sub>O<sub>4</sub> nanotheranostic for magnetically targeted photothermal therapy guided by magnetic resonance/ photoacoustic imaging. *Theranostics*. 2015; 5: 931-45.
95. Zhang W, Shi S, Wang Y, Yu S, Zhu W, Zhang X, et al. Versatile molybdenum disulfide based antibacterial composites for *in vitro* enhanced sterilization and *in vivo* focal infection therapy. *Nanoscale*. 2016; 8: 11642-8.
96. Liu Y, Zeng X, Hu X, Hua J, Zhang X. Two-dimensional nanomaterials for photocatalytic water disinfection: recent progress and future challenges. *J Chem Technol Biotechnol*. 2019; 94: 22-37.
97. Liu C, Kong D, Hsu PC, Yuan H, Lee HW, Liu Y, et al. Rapid water disinfection using vertically aligned MoS<sub>2</sub> nanofilms and visible light. *Nat Nanotechnol*. 2016; 11: 1098-105.
98. Wu D, Wang B, Wang W, An T, Li G, Ng TW, et al. Visible-light-driven BiOBr nanosheets for highly facet-dependent photocatalytic inactivation of *Escherichia coli*. *J Mater Chem A*. 2015; 3: 15148-55.
99. Wu D, Yue S, Wang W, An T, Li G, Yip HY, et al. Boron doped BiOBr nanosheets with enhanced photocatalytic inactivation of *Escherichia coli*. *Appl Catal B*. 2016; 192: 35-45.
100. Wu D, Yue S, Wang W, An T, Li G, Ye L, et al. Influence of photoinduced Bi-related self-doping on the photocatalytic activity of BiOBr nanosheets. *Appl Surf Sci*. 2017; 391: 516-24.
101. Wu D, Ye L, Yue S, Wang B, Wang W, Yip HY, et al. Alkali-induced *in situ* fabrication of Bi<sub>2</sub>O<sub>3</sub>-decorated BiOBr nanosheets with excellent photocatalytic performance. *J Phys Chem C*. 2016; 120: 7715-27.
102. Murugesan P, Moses JA, Anandharamkrishnan C. Photocatalytic disinfection efficiency of 2D structure graphitic carbon nitride-based nanocomposites: a review. *J Mater Sci*. 2019; 54: 12206-35.
103. Cao S, Low J, Yu J, Jaroniec M. Polymeric Photocatalysts Based on Graphitic Carbon Nitride. *Adv Mater*. 2015; 27: 2150-76.
104. Adhikari SP, Awasthi GP, Lee J, Park CH, Kim CS. Synthesis, characterization, organic compound degradation activity and antimicrobial performance of g-C<sub>3</sub>N<sub>4</sub> sheets customized with metal nanoparticles-decorated TiO<sub>2</sub> nanofibers. *RSC Adv*. 2016; 6: 55079-91.
105. Huang J, Ho W, Wang X. Metal-free disinfection effects induced by graphitic carbon nitride polymers under visible light illumination. *Chem Commun*. 2014; 50: 4338-40.
106. Zhao H, Yu H, Quan X, Chen S, Zhang Y, Zhao H, et al. Fabrication of atomic single layer graphitic-C<sub>3</sub>N<sub>4</sub> and its high performance of photocatalytic disinfection under visible light irradiation. *Appl Catal B*. 2014; 152-153: 46-50.
107. Liu B, Han X, Wang Y, Fan X, Wang Z, Zhang J, et al. Synthesis of g-C<sub>3</sub>N<sub>4</sub>/BiOI/BiOBr heterostructures for efficient visiblelight-induced photocatalytic and antibacterial activity. *J Mater Sci: Mater Electron*. 2018; 29: 14300-10.
108. Jia Y, Zhan S, Ma S, Zhou Q. Fabrication of TiO<sub>2</sub>-Bi<sub>2</sub>WO<sub>6</sub> binanosheet for enhanced solar photocatalytic disinfection of *E. coli*: insights on the mechanism. *ACS Appl Mater Interfaces*. 2016; 8: 6841-51.
109. Tian X, Sun Y, Fan S, Boudreau MD, Chen C, Ge C, et al. Photogenerated Charge Carriers in Molybdenum Disulfide Quantum Dots with Enhanced Antibacterial Activity. *ACS Appl Mater Interfaces*. 2019; 11: 4858-66.
110. Adhikari SP, Pant HR, Kim JH, Kim HJ, Park CH, Kim CS. One pot synthesis and characterization of Ag-ZnO/g-C<sub>3</sub>N<sub>4</sub> photocatalyst with improved photoactivity and antibacterial properties. *Colloids Surf, A Physicochem Eng Asp*. 2015; 482: 477-84.
111. Zhao H, Chen S, Quan X, Yu H, Zhao H. Integration of microfiltration and visible-light-driven photocatalysis on g-C<sub>3</sub>N<sub>4</sub> nanosheet/reduced graphene oxide membrane for enhanced water treatment. *Appl Catal B*. 2016; 194: 134-40.
112. Wang Y, Long Y, Zhang D. Novel bifunctional V<sub>2</sub>O<sub>5</sub>/BiVO<sub>4</sub> nanocomposite materials with enhanced antibacterial activity. *J Taiwan Inst Chem Eng*. 2016; 68: 387-95.
113. Wang W, Yu JC, Xia D, Wong PK, Li Y. Graphene and g-C<sub>3</sub>N<sub>4</sub> nanosheets cowrapped elemental α-Sulfur as a novel metal-free heterojunction photocatalyst for bacterial inactivation under visible-light. *Environ Sci Technol*. 2013; 47: 8724-32.
114. Xu J, Li Y, Zhou X, Li Y, Gao Z, Song Y, et al. Graphitic C<sub>3</sub>N<sub>4</sub>-sensitized TiO<sub>2</sub> nanotube layers: a visible-light activated efficient metal-free antimicrobial platform. *Chemistry*. 2016; 22: 3947-51.
115. Li J, Yin Y, Liu E, Ma Y, Wan J, Fana J, et al. *In situ* growing Bi<sub>2</sub>MoO<sub>6</sub> on g-C<sub>3</sub>N<sub>4</sub> nanosheets with enhanced photocatalytic hydrogen evolution and disinfection of bacteria under visible light irradiation. *J Hazard Mater*. 2017; 321: 183-92.
116. De Melo WC, Avci P, de Oliveira MN, Gupta A, Vecchio D, Sadasivam M, et al. Photodynamic inactivation of biofilm: taking a lightly colored approach to stubborn infection. *Expert Rev Anti Infect Ther*. 2013; 11: 669-93.
117. Abrahamse H, Hamblin MR. New photosensitizers for photodynamic therapy. *Biochem J*. 2016; 473: 347-64.
118. Chilakamarthi U, Giribabu L. Photodynamic therapy: past, present and future. *Chem Rec*. 2017; 17: 775-802.
119. Fan W, Huang P, Chen X. Overcoming the Achilles' heel of photodynamic therapy. *Chem Soc Rev*. 2016; 45: 6488-519.
120. Biel MA. Photodynamic therapy of bacterial and fungal biofilm infections. Totowa, NJ: Humana Press; 2010: 175-194.
121. Jia Q, Song Q, Li P, Huang W. Rejuvenated Photodynamic Therapy for Bacterial Infections. *Adv Healthc Mater*. 2019; 8: e1900608.
122. Tan L, Li J, Liu X, Cui Z, Yang X, Yeung KWK, et al. *In situ* disinfection through photoinspired radical oxygen species storage and thermal-triggered release from black phosphorous with strengthened chemical stability. *Small*. 2018; 14: 1703197.
123. Richter AP, Brown JS, Bharti B, Wang A, Gangwal S, Houck K, et al. An environmentally benign antimicrobial nanoparticle based on a silver-infused lignin core. *Nat Nanotechnol*. 2015; 10: 817-23.
124. Zhang Q, Sun C, Zhao Y, Zhou S, Hu X, Chen P. Low Ag-doped titanium dioxide nanosheet films with outstanding antimicrobial property. *Environ Sci Technol*. 2010; 44: 8270-5.
125. Ali SR, Pandit S, De M. 2D-MoS<sub>2</sub>-based β-Lactamase inhibitor for combination therapy against drug-resistant bacteria. *ACS Appl Bio Mater*. 2018; 1: 967-74.
126. Ryu SJ, Jung H, Oh JM, Lee JK, Choy JH. Layered double hydroxide as novel antibacterial drug delivery system. *J Phys Chem Solids*. 2010; 71: 685-8.
127. Zhang X, Zhang W, Liu L, Yang M, Huang L, Chen K, et al. Antibiotic-loaded MoS<sub>2</sub> nanosheets to combat bacterial resistance *via* biofilm inhibition. *Nanotechnology*. 2017; 28: 225101-12.
128. Singh AK, Mishra H, Firdaus Z, Yadav S, Aditi P, Nandy N, et al. MoS<sub>2</sub>-modified curcumin nanostructures: the novel theranostic hybrid having potent antibacterial and antibiofilm activities against multidrug-resistant hypervirulent klebsiella pneumoniae. *Chem Res Toxicol*. 2019; 8: 1599-618.
129. Feng Q, Wu J, Chen G, Cui F, Kim TN, Kim JO. A mechanistic study of the antibacterial effect of silver ions on *Escherichia coli* and *Staphylococcus aureus*. *J Biomed Mater Res*. 2000; 52: 662-8.
130. Sondi I, Salopek-Sondi B. Silver nanoparticles as antimicrobial agent: a case study on *E. coli* as a model for Gram-negative bacteria. *J Colloid Interface Sci*. 2004; 275: 177-82.
131. Chernousova S, Epple M. Silver as antibacterial agent: ion, nanoparticle, and metal. *Angew Chem Int Ed*. 2013; 52: 1636-53.
132. Yu S, Li G, Liu R, Ma D, Xue W. Dendritic Fe<sub>3</sub>O<sub>4</sub>@Poly(dopamine)@PAMAM nanocomposite as controllable NO-releasing material: a synergistic photothermal and NO antibacterial study. *Adv Funct Mater*. 2018; 1707440-54.
133. Wu J, Li Y, He C, Kang J, Ye J, Xiao Z, et al. Novel H<sub>2</sub>S releasing nanofibrous coating for *In Vivo* dermal wound regeneration. *ACS Appl Mater Interfaces*. 2016; 8: 27474-81.
134. Xu Z, Qiu Z, Liu Q, Huang Y, Li D, Shen X, et al. Converting organosulfur compounds to inorganic polysulfides against resistant bacterial infections. *Nat Commun*. 2018; 9: 3713-26.
135. Xu Y, Li S, Yue X, Lu W. Review of silver nanoparticles (AgNPs)-cellulose antibacterial composites. *Bioresources*. 2018; 13: 2150-70.
136. Cao F, Ju E, Zhang Y, Wang Z, Liu C, Li W, et al. An efficient and benign antimicrobial depot based on silver-infused MoS<sub>2</sub>. *ACS Nano*. 2017; 11: 4651-9.
137. Zhou F, Mei L, Lei T, Duo C, Jin Y, Yang L, et al. Electrophoretic deposited stable chitosan@MoS<sub>2</sub> coating with rapid *in situ* bacteria-killing ability under dual-light irradiation. *Small*. 2018; 14: 1704347.
138. Zhang X, Zhang C, Yang Y, Zhang H, Huang X, Hang R, et al. Light-assisted rapid sterilization by a hydrogel incorporated with Ag<sub>3</sub>PO<sub>4</sub>/MoS<sub>2</sub> composites for efficient wound disinfection. *Chem Eng J*. 2019; 374: 596-604.
139. Li Y, Liu X, Tan L, Cui Z, Yang X, Zheng Y, et al. Rapid Sterilization and Accelerated Wound Healing Using Zn<sup>2+</sup> and Graphene Oxide Modified g-C<sub>3</sub>N<sub>4</sub> under Dual Light Irradiation. *Adv Funct Mater*. 2018; 28: 1800299.
140. Zhang C, Hu D, Xu J, Ma M, Xing H, Yao K, et al. Polyphenol-assisted exfoliation of transition metal dichalcogenides into nanosheets as photothermal nanocarriers for enhanced antibiofilm activity. *ACS Nano*. 2018; 12: 12347-56.
141. Lin Y, Han D, Li Y, Tan L, Liu X, Cui Z, et al. Ag<sub>2</sub>S@WS<sub>2</sub> Heterostructure for Rapid Bacteria-Killing Using Near-Infrared Light. *ACS Sustainable Chem Eng*. 2019; 7: 14982-90.
142. Li B, Tan L, Liu X, Li Z, Cui Z, Liang Y, et al. Superimposed surface plasma resonance effect enhanced the near-infrared photocatalytic activity of Au@Bi<sub>2</sub>WO<sub>6</sub> coating for rapid bacterial killing. *J Hazard Mater*. 2019; 380: 120818.
143. Yin W, Yu J, Lv F, Yan L, Zheng L, Gu Z, et al. Functionalized nano-MoS<sub>2</sub> with peroxidase catalytic and near-infrared photothermal activities for safe and synergetic wound antibacterial applications. *ACS Nano*. 2016; 10: 11000-11.
144. Cao F, Zhang L, Wang H, You Y, Wang Y, Gao N, et al. Defect-rich adhesive nanozymes as efficient "antibiotics" for enhanced bacterial inhibition. *Angew Chem Int Ed*. 2019; DOI:10.1002/anie.201908289.
145. Yin Q, Tan L, Lang Q, Ke X, Bai L, Guo K, et al. Plasmonic molybdenum oxide nanosheets supported silver nanocubes for enhanced near-infrared antibacterial activity: Synergism of photothermal effect, silver release and photocatalytic reactions. *Appl Catal B*. 2018; 224: 671-80.
146. Roy S, Mondal A, Yadav V, Sarkar A, Banerjee R, Sanpui P, et al. Mechanistic insight into the antibacterial activity of chitosan exfoliated MoS<sub>2</sub> nanosheets: membrane damage, metabolic inactivation, and oxidative stress. *ACS Appl Bio Mater*. 2019; 2: 2738-55.
147. Li M, Li L, Su K, Liu X, Zhang T, Liang Y, et al. Highly effective and noninvasive near-infrared eradication of a *Staphylococcus aureus* biofilm on implants by a photoresponsive coating within 20 min. *Adv Sci*. 2019; 1900599.
148. Yuwen L, Sun Y, Tan G, Xiu W, Zhang Y, Weng L, et al. MoS<sub>2</sub>@polydopamine-Ag nanosheets with enhanced antibacterial activity for effective treatment of *Staphylococcus aureus* biofilms and wound infection. *Nanoscale*. 2018; 10: 16711-20.

149. Lok C, Ho C, Chen R, He Q, Yu W, Sun H, et al. Silver nanoparticles: partial oxidation and antibacterial activities. *J Biol Inorg Chem*. 2007; 12: 527-34.
150. Chen C, Gunawan P, Lou X, Xu R. Silver nanoparticles deposited layered double hydroxide nanoporous coatings with excellent antimicrobial activities. *Adv Funct Mater*. 2012; 22: 780-7.
151. Tang S, Zheng J. Antibacterial activity of silver nanoparticles: structural effects. *Adv Healthc Mater*. 2018; 7: 1701503.
152. Ananth A, Dharaneedharan S, Gandhi MS, Heo MS, Mok YS. Novel RuO<sub>2</sub> nanosheets-Facile synthesis, characterization and application. *Chem Eng J*. 2013; 223: 729-36.
153. Sun Z, Zhang Y, Yu H, Yan C, Liu Y, Hong S, et al. New solvent-stabilized few-layer black phosphorus for antibacterial applications. *Nanoscale*. 2018; 10: 12543-53.
154. Kan M, Wang J, Li X, Zhang S, Li Y, Kawazoe Y, et al. Structures and phase transition of a MoS<sub>2</sub> monolayer. *J Phys Chem C*. 2014; 118: 1515-22.
155. Ke Y, Liu C, Zhang X, Xiao M, Wu G. Surface Modification of Polyhydroxyalkanoates toward Enhancing Cell Compatibility and Antibacterial Activity. *Macromol Mater Eng*. 2017; 302: 1700258.
156. Cao W, Yue L, Wang Z. High antibacterial activity of chitosan-molybdenum disulfide nanocomposite. *Carbohydr Polym*. 2019; 215: 226-34.
157. Gao Q, Zhang X, Yin W, Ma D, Xie C, Zheng L, et al. Functionalized MoS<sub>2</sub> nanovehicle with near-infrared laser-mediated nitric oxide release and photothermal activities for advanced bacteria-infected wound therapy. *Small*. 2018; 0: 1802290-305.
158. Cheng P, Zhou Q, Hu X, Su S, Wang X, Jin M, et al. Transparent glass with growth of pyramid-type MoS<sub>2</sub> for highly efficient water disinfection under visible light irradiation. *ACS Appl Mater Interfaces*. 2018; 10: 23444-50.
159. Huang X, Wei J, Liu T, Zhang X, Bai S, Yang H. Silk fibroin-assisted exfoliation and functionalization of transition metal dichalcogenide nanosheets for antibacterial wound dressings. *Nanoscale*. 2017; 9: 17193-8.
160. Masimukub S, Hub YC, Linc ZH, Chanc SW, Chouc TM, Wu JM. High efficient degradation of dye molecules by PDMS embedded abundant single-layer tungsten disulfide and their antibacterial performance. *Nano Energy*. 2018; 46: 338-46.
161. Kumar P, Kataria S, Roy S, Jaiswal A, Balakrishnan V. Photocatalytic water disinfection of CVD grown WS<sub>2</sub> monolayer decorated with Ag nanoparticles. *ChemistrySelect*. 2018; 3: 7648-55.
162. Mo S, Chen X, Chen M, He C, Lu Y, Zheng N. Two-dimensional antibacterial Pd@Ag nanosheets with a synergetic effect of plasmonic heating and Ag<sup>+</sup> release. *J Mater Chem B*. 2015; 3: 6255-60.
163. Wang X, Su K, Tan L, Liu X, Cui Z, Jing D, et al. Rapid and highly effective noninvasive disinfection by hybrid Ag/CS@MnO<sub>2</sub> nanosheets using near-infrared light. *ACS Appl Mater Interfaces*. 2019; 11: 15014-27.
164. Kaushik R, Vineeth Daniel P, Mondal P, Halder A. Transformation of 2-D TiO<sub>2</sub> to mesoporous hollow 3-D TiO<sub>2</sub> spheres-comparative studies on morphology-dependent photocatalytic and anti-bacterial activity. *Microporous Mesoporous Mater*. 2019; 285: 32-42.
165. Pal A, Jana TK, Roy T, Pradhan A, Maiti R, M. Choudhury S, et al. MoS<sub>2</sub>-TiO<sub>2</sub> nanocomposite with excellent adsorption performance and high antibacterial activity. *ChemistrySelect*. 2018; 3: 81-90.
166. Li R, Ren Y, Zhao P, Wang J, Liu J, Zhang Y. Graphitic carbon nitride (g-C<sub>3</sub>N<sub>4</sub>) nanosheets functionalized composite membrane with self-cleaning and antibacterial performance. *J Hazard Mater*. 2019; 365: 606-14.
167. Dai J, Song J, Qiu Y, Wei J, Hong Z, Li L, et al. Gold nanoparticle-decorated g-C<sub>3</sub>N<sub>4</sub> nanosheets for controlled generation of reactive oxygen species upon 670 nm laser illumination. *ACS Appl Mater Interfaces*. 2019; 11: 10589-96.
168. Liu C, Wang L, Xu H, Wang S, Gao S, Ji X, et al. "One pot" green synthesis and the antibacterial activity of g-C<sub>3</sub>N<sub>4</sub>/Ag nanocomposites. *Mater Lett*. 2016; 164: 567-70.
169. Khan ME, Han TH, Khan MM, Karim MR, Cho MH. Environmentally sustainable fabrication of Ag@g-C<sub>3</sub>N<sub>4</sub> nanostructures and their multifunctional efficacy as antibacterial agents and photocatalysts. *ACS Appl Nano Mater*. 2018; 1: 2912-22.
170. Wu Y, Zhou Y, Xu H, Liu Q, Li Y, Zhang L, et al. Highly active, superstable, and biocompatible Ag/polydopamine/g-C<sub>3</sub>N<sub>4</sub> bactericidal photocatalyst: synthesis, characterization, and mechanism. *ACS Sustainable Chem Eng*. 2018; 6: 14082-94.
171. Wang R, Kong X, Zhang W, Zhu W, Huang L, Wang J, et al. Mechanism insight into rapid photocatalytic disinfection of salmonella based on vanadate QDs-interspersed g-C<sub>3</sub>N<sub>4</sub> heterostructures. *Appl Catal B*. 2018; 225: 228-37.
172. Wu Q, Liang M, Zhang S, Liu X, Wang F. Development of functional black phosphorus nanosheets with remarkable catalytic and antibacterial performance. *Nanoscale*. 2018; 10: 10428-35.
173. Rasool K, Helal M, Ali A, Ren CE, Gogotsi Y, Mahmoud KA. Antibacterial activity of Ti<sub>3</sub>C<sub>2</sub>T<sub>x</sub> MXene. *ACS Nano*. 2016; 10: 3674-84.
174. Rasool K, Mahmoud KA, Johnson DJ, Helal M, Berdiyrov GR, Gogotsi Y. Efficient antibacterial membrane based on two-dimensional Ti<sub>3</sub>C<sub>2</sub>T<sub>x</sub> (MXene) nanosheets. *Sci Rep*. 2017; 7: 1598-609.
175. Wang Z, Yu H, Ma K, Chen Y, Zhang X, Wang T, et al. Flower-like surface of three-metal-component layered double hydroxide composites for improved antibacterial activity of lysozyme. *Bioconjugate Chem*. 2018; 29: 2090-9.
176. Gao G, Mathkar A, Martins EP, Galvão DS, Gao D, Autreto PAdS, et al. Designing nanoscaled hybrids from atomic layered boron nitride with silver nanoparticle deposition. *J Mater Chem A*. 2014; 2: 3148-54.
177. Zhu C, Shen H, Liu H, Lv X, Li Z, Yuan Q. Solution-processable two-dimensional In<sub>2</sub>Se<sub>3</sub> nanosheets as efficient photothermal agents for elimination of bacteria. *Chemistry*. 2018; 24: 19060-5.
178. Li X, Shan J, Zhang W, Su S, Yuwen L, Wang L. Recent advances in synthesis and biomedical applications of two-dimensional transition metal dichalcogenide nanosheets. *Small*. 2017; 13: 1602660-88.
179. Kalantar zadeh K, Ou JZ, Daeneke T, Strano MS, Pumera M, Gras SL. Two-dimensional transition metal dichalcogenides in biosystems. *Adv Funct Mater*. 2015; 25: 5086-99.
180. Zhang B, Zou S, Cai R, Li M, He Z. Highly-efficient photocatalytic disinfection of *Escherichia coli* under visible light using carbon supported Vanadium Tetrasulfide nanocomposites. *Appl Catal B*. 2018; 224: 383-93.
181. Yong Y, Cheng X, Bao T, Zu M, Yan L, Yin W, et al. Tungsten sulfide quantum dots as multifunctional nanotheranostics for *in vivo* dual-modal image-guided photothermal/radiotherapy synergistic therapy. *ACS Nano*. 2015; 9: 12451-63.
182. Dong X, Yin W, Zhang X, Zhu S, He X, Yu J, et al. Intelligent MoS<sub>2</sub> nanotheranostic for targeted and enzyme-/pH-/NIR-responsive drug delivery to overcome cancer chemotherapy resistance guided by PET imaging. *ACS Appl Mater Interfaces*. 2018; 10: 4271-84.
183. Yang L, Wang J, Yang S, Lu Q, Li P, Li N. Rod-shape MSN@MoS<sub>2</sub> Nanoplatfor for FL/MSOT/CT Imaging-Guided Photothermal and Photodynamic Therapy. *Theranostics*. 2019; 9: 3992-4005.
184. Wu N, Yu Y, Li T, Ji X, Jiang L, Zong J, et al. Investigating the influence of MoS<sub>2</sub> nanosheets on *E. coli* from metabolomics level. *PLoS One*. 2016; 11: e0167245.
185. Niu J, Sun Y, Wang F, Zhao C, Ren J, Qu X. Photomodulated nanozyme used for a gram-selective antimicrobial. *Chem Mater*. 2018; 30: 7027-33.
186. Fakhri A, Gupta VK, Rabizadeh H, Agarwal S, Sadeghi N, Tahami S. Preparation and characterization of WS<sub>2</sub> decorated and immobilized on chitosan and polycaprolactone as biodegradable polymers nanofibers: Photocatalysis study and antibiotic-conjugated for antibacterial evaluation. *Int J Biol Macromol*. 2018; 120: 1789-93.
187. Li J, Cha R, Zhao X, Guo H, Luo H, Wang M, et al. Gold nanoparticles cure bacterial infection with benefit to intestinal microflora. *ACS Nano*. 2019; 13: 5002-14.
188. Shahmiri M, Ibrahim N, Shayesteh F, Asim N, Motallebi N. Preparation of PVP-coated copper oxide nanosheets as antibacterial and antifungal agents. *J Mater Res*. 2013; 28: 3109-18.
189. Raghupathi KR, Koodali RT, Manna AC. Size-dependent bacterial growth inhibition and mechanism of antibacterial activity of zinc oxide nanoparticles. *Langmuir*. 2011; 27: 4020-8.
190. Li Y, Liu G, Zhai Z, Liu L, Li H, Yang K, et al. Antibacterial properties of magnesium *in vitro* and in an *in vivo* model of implant-associated methicillin-resistant *Staphylococcus aureus* infection. *Antimicrob Agents Chemother*. 2014; 58: 7586-91.
191. Robinson DA, Griffith RW, Shechtman D, Evans RB, Conzemius MG. *In vitro* antibacterial properties of magnesium metal against *Escherichia coli*, *Pseudomonas aeruginosa* and *Staphylococcus aureus*. *Acta Biomater*. 2010; 6: 1869-77.
192. Behin J, Shahryarifar A, Kazemian H. Ultrasound-assisted synthesis of Cu and Cu/Ni nanoparticles on NaP zeolite support as antibacterial agents. *Chem Eng Technol*. 2016; 39: 2389-403.
193. Chondath SK, Poolakkandy RR, Kottayintavida R, Thekkangil A, Gopalan NK, Vasu ST, et al. Water-Chloroform Interface Assisted Microstructure Tuning of Polypyrrole-Silver Sheets. *ACS Appl Mater Interfaces*. 2019; 11: 1723-31.
194. Song X, Hu J, Zeng H. Two-dimensional semiconductors: recent progress and future perspectives. *J Mater Chem C*. 2013; 1: 2952-69.
195. Wang G, Xing Z, Zeng X, Feng C, McCarthy DT, Deletic A, et al. Ultrathin titanium oxide nanosheets film with memory bactericidal activity. *Nanoscale*. 2016; 8: 18050-6.
196. Wang B, Leung MKH, Lu X, Chen S. Synthesis and photocatalytic activity of boron and fluorine codoped TiO<sub>2</sub> nanosheets with reactive facets. *Appl Energy*. 2013; 112: 1190-7.
197. Zanni E, Chandriaahgari RC, De Bellis G, Montereali RM, Armiento G, Ballirano P, et al. Zinc oxide nanorods-decorated graphene nanoplatelets: a promising antimicrobial agent against the cariogenic bacterium streptococcus mutans. *Nanomaterials*. 2016; 6: 179-93.
198. He W, Kim HK, Wamer WG, Melka D, Callahan JH, Yin J. Photogenerated charge carriers and reactive oxygen species in ZnO/Au hybrid nanostructures with enhanced photocatalytic and antibacterial activity. *J Am Chem Soc*. 2014; 136: 750-7.
199. Ma S, Zhan S, Jia Y, Zhou Q. Superior antibacterial activity of Fe<sub>3</sub>O<sub>4</sub>-TiO<sub>2</sub> nanosheets under solar light. *ACS Appl Mater Interfaces*. 2015; 7: 21875-83.
200. Ong WJ, Tan LL, Ng YH, Yong ST, Chai SP. Graphitic carbon nitride (g-C<sub>3</sub>N<sub>4</sub>)-based photocatalysts for artificial photosynthesis and environmental remediation: are we a step closer to achieving sustainability? *Chem Rev*. 2016; 116: 7159-329.
201. Wang L, Zhang X, Yu X, Gao F, Shen Z, Zhang X, et al. An all-organic semiconductor C<sub>3</sub>N<sub>4</sub>/PDINH heterostructure with advanced antibacterial photocatalytic therapy activity. *Adv Mater*. 2019; 0: 1901965.
202. Li Z, Wu L, Wang H, Zhou W, Liu H, Cui H, et al. Synergistic antibacterial activity of black phosphorus nanosheets modified with titanium aminobenzenesulfanato complexes. *ACS Appl Nano Mater*. 2019; 2: 1202-9.

203. Lei W, Liu G, Zhang J, Liu M. Black phosphorus nanostructures: recent advances in hybridization, doping and functionalization. *Chem Soc Rev.* 2017; 46: 3492-509.
204. Luo M, Fan T, Zhou Y, Zhang H, Mei L. 2D black phosphorus-based biomedical applications. *Adv Funct Mater.* 2019; 29: 1808306.
205. Choi JR, Yong KW, Choi JY, Nilghaz A, Lin Y, Xu J, et al. Black Phosphorus and its Biomedical Applications. *Theranostics.* 2018; 8: 1005-26.
206. Ge X, Xia Z, Guo S. Recent advances on black phosphorus for biomedicine and biosensing. *Adv Funct Mater.* 2019; 29: 1900318.
207. Ouyang J, Liu R, Chen W, Liu Z, Xu Q, Zeng K, et al. A black phosphorus based synergistic antibacterial platform against drug resistant bacteria. *J Mater Chem B.* 2018; 6: 6302-10.
208. Liu G, Shen J, Ji Y, Liu Q, Liu G, Yang J, et al. Two-dimensional Ti<sub>2</sub>CT<sub>x</sub>MXene membranes with integrated and ordered nanochannels for efficient solvent dehydration. *J Mater Chem A.* 2019; 7: 12095-104.
209. Anasori B, Lukatskaya MR, Gogotsi Y. 2D metal carbides and nitrides (MXenes) for energy storage. *Nat Rev Mater.* 2017; 2: 16098.
210. Lin H, Chen Y, Shi J. Insights into 2D MXenes for versatile biomedical applications: current advances and challenges ahead. *Adv Sci.* 2018; 5: 1800518.
211. Han X, Jing X, Yang D, Lin H, Wang Z, Ran H, et al. Therapeutic mesopore construction on 2D Nb<sub>2</sub>C MXenes for targeted and enhanced chemo-photothermal cancer therapy in NIR-II biowindow. *Theranostics.* 2018; 8: 4491-508.
212. Arabi Shamsabadi A, Sharifian Gh M, Anasori B, Soroush M. Antimicrobial mode-of-action of colloidal Ti<sub>3</sub>C<sub>2</sub>T<sub>x</sub> MXene nanosheets. *ACS Sustainable Chem Eng.* 2018; 6: 16586-96.
213. Mishra G, Dash B, Pandey S, Mohanty PP. Antibacterial actions of silver nanoparticles incorporated Zn-Al layered double hydroxide and its spinel. *J Environ Chem Eng.* 2013; 1: 1124-30.
214. Yang Q, Chang Y, Zhao H. Preparation and antibacterial activity of lysozyme and layered double hydroxide nanocomposites. *Water Res.* 2013; 47: 6712-8.
215. Wang Q, O'Hare D. Recent advances in the synthesis and application of layered double hydroxide (LDH) nanosheets. *Chem Rev.* 2012; 112: 4124-55.
216. Mishra G, Dash B, Pandey S. Layered double hydroxides: A brief review from fundamentals to application as evolving biomaterials. *Appl Clay Sci.* 2018; 153: 172-86.
217. Leon Morales CF, Leis AP, Strathmann M, Flemming HC. Interactions between laponite and microbial biofilms in porous media: implications for colloid transport and biofilm stability. *Water Res.* 2004; 38: 3614-26.
218. Das SS, Neelam, Hussain K, Singh S, Hussain A, Faruk A, et al. Laponite-based nanomaterials for biomedical applications: a review. *Curr Pharm Des.* 2019; 25: 424-43.
219. Ding W, Zhu J, Wang Z, Gao Y, Xiao D, Gu Y, et al. Prediction of intrinsic two-dimensional ferroelectrics in In<sub>2</sub>Se<sub>3</sub> and other III<sub>2</sub>-VI<sub>3</sub> van der Waals materials. *Nat Commun.* 2017; 8: 14956-64.
220. Gorle G, Bathinapatla A, Chen Y, Ling Y. Near infrared light activatable PEI-wrapped bismuth selenide nanocomposites for photothermal/photodynamic therapy induced bacterial inactivation and dye degradation. *RSC Adv.* 2018; 8: 19827-34.
221. Ghadiri M, Chrzanowski W, Rohanizadeh R. Antibiotic eluting clay mineral (Laponite(R)) for wound healing application: an *in vitro* study. *J Mater Sci Mater Med.* 2014; 25: 2513-26.
222. Zhao F, Zhao Y, Liu Y, Chang X, Chen C, Zhao Y. Cellular uptake, intracellular trafficking, and cytotoxicity of nanomaterials. *Small.* 2011; 7: 1322-37.
223. Mei L, Zhang X, Yin W, Dong X, Guo Z, Fu W, et al. Translocation, biotransformation-related degradation, and toxicity assessment of polyvinylpyrrolidone-modified 2H-phase nano-MoS<sub>2</sub>. *Nanoscale.* 2019; 11: 4767-80.
224. Hussain SM, Stolle LKB, Schrand AM, Murdock RC, Yu KO, Mattie DM, et al. Toxicity evaluation for safe use of nanomaterials: recent achievements and technical challenges. *Adv Mater.* 2009; 21: 1549-59.
225. Feng Q, Liu Y, Huang J, Chen K, Huang J, Xiao K. Uptake, distribution, clearance, and toxicity of iron oxide nanoparticles with different sizes and coatings. *Sci Rep.* 2018; 8: 2082-94.
226. Li Z, Zhang Y, Ma J, Meng Q, Fan J. Modeling Interactions between Liposomes and Hydrophobic Nanosheets. *Small.* 2019; 15: 1804992.